Finite temperature QCD phase transition with 3 flavors of Möbius domain wall fermions

Yu Zhang

Bielefeld University

In collaboration with

Y. Aoki, S. Hashimoto, I. Kanamori, T. Kaneko, Y. Nakamura

New developments in studies of the QCD phase diagram
ECT* Trento, Sep 9-13, 2024

The nature of QCD phase transition at $\mu_B = 0$

Columbia plot

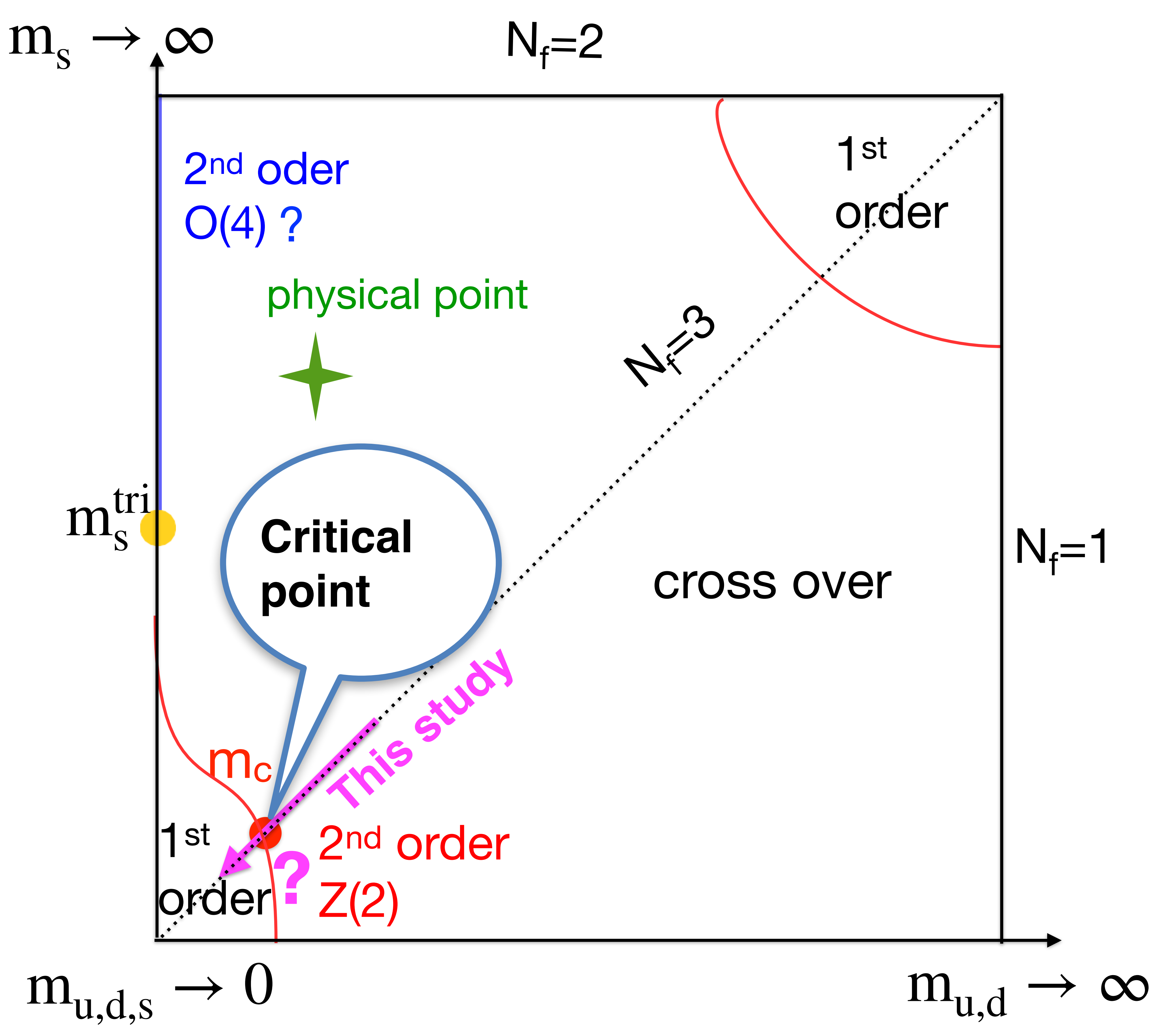

- ϵ expansion: 1^{st} order phase transition in the chiral limit for $N_f = 3$

  [R. D. Pisarski, F. Wilczek PRD 84]

- Possible 2^{nd} order phase transition in the $N_f = 3$ chiral limit:

  [G. Fejos, PRD 22]
  [S. R. Kousvos, A. Stergiou SciPost 23]
  [J. Bernhardt, C. S. Fischer PRD 23]
  [R. D. Pisarski, F. Rennecke PRL 24]
  [G. Fejos, T. Hatsuda PRD 24]

[talk by R.D. Pisarki on Wed.]

Need to be checked by lattice QCD

Critical point on the $N_f = 3$ chiral region:

- ❑ Location? (existence?)
- ❑ Universality class?

Previous Nf=3 lattice QCD studies

Action	N_t	$m_\pi^{Z_2}$ [MeV]	Ref.
Staggered,standard	4	290	Karsch et al. (2001)
Staggered,standard	6	150	de Forcrand et al. (2007)
Staggered, HISQ	6	$\lesssim 50$	Bazavov et al. (2017)
Staggered, stout	4-6	0?	Varnhost (2014)
Wilson, standard	4	$\lesssim 670$	Iwasaki et al. (1996)
Wilson-Clover	6-10	$\lesssim 170$	Jin et al. (2017)
Wilson-Clover	6-12	$\lesssim 110$	Kuramashi et al. (2020)

➡ Strong cutoff and discretization effects

Evidence for chiral limit to feature 2nd order PT with staggered and HISQ fermion [F. Cuteri et al. JHEP 2021; S. Sharma et al. PRD 2022]

[talk by O. Philipsen on Wed.]

We propose to use chiral fermion (Mobius domain wall fermion)

- Exact chiral symmetry at finite a for infinite Ls
- Reduced χ_{SB} parameterized by residual mass when Ls is finite

Lattice Setup

- N_f=3 Mobius Domain Wall Fermion
- Tree-level Symanzik improved gauge action and stout smearing

☆T=0:

$$\beta = 4.0, 24^3 \times 48 \times 16 : \quad 0.02 \leq am_q \leq 0.045,\ am_{\text{res}}(\text{estimated}) \approx 0.006$$

$$\beta = 4.1, 24^3 \times 48 \times 16 : \quad 0.015 \leq am_q \leq 0.040$$

$$\beta = 4.17, 32^3 \times 64 \times 16 : \quad 0.012 \leq am_q \leq 0.026$$

☆T=121(2) MeV ($\beta = 4.0$, ($a = 0.1361(20)$ fm, determined from Wilson flow t_0))

$$N_s^3 \times 12 \times 16 : \quad N_s = 48, -0.004 \leq am_q \leq -0.003$$

$$N_s = 36, -0.005 \leq am_q \leq 0.001$$

$$N_s = 24, -0.006 \leq am_q \leq 0.1$$

$$N_s^3 \times 12 \times 32 : \quad N_s = 24, -0.001 \leq am_q \leq 0.003$$

Residual chiral symmetry breaking

$$m_{\rm res} = \left. \frac{\left\langle \sum_{\vec{x}} J^a_{5q}(\vec{x},t) P^a(\vec{0},0) \right\rangle}{\left\langle \sum_{\vec{x}} P^a(\vec{x},t) P^a(\vec{0},0) \right\rangle} \right|_{t \geq t_{min}}$$

- **For finite Ls chiral symmetry is broken, leading to an additive renormalization of the mass:** $m_q \to m_q + m_{\rm res}$

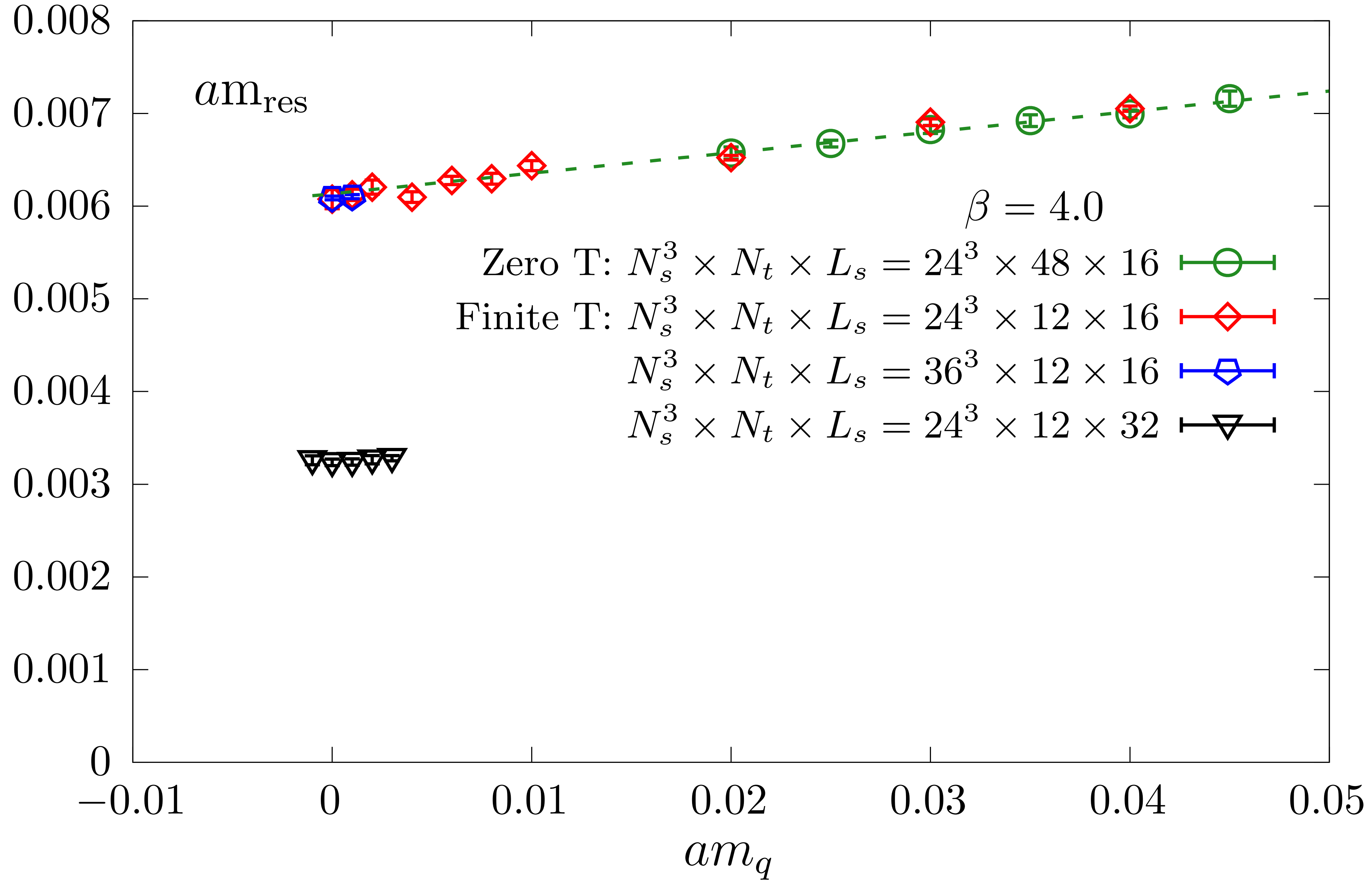

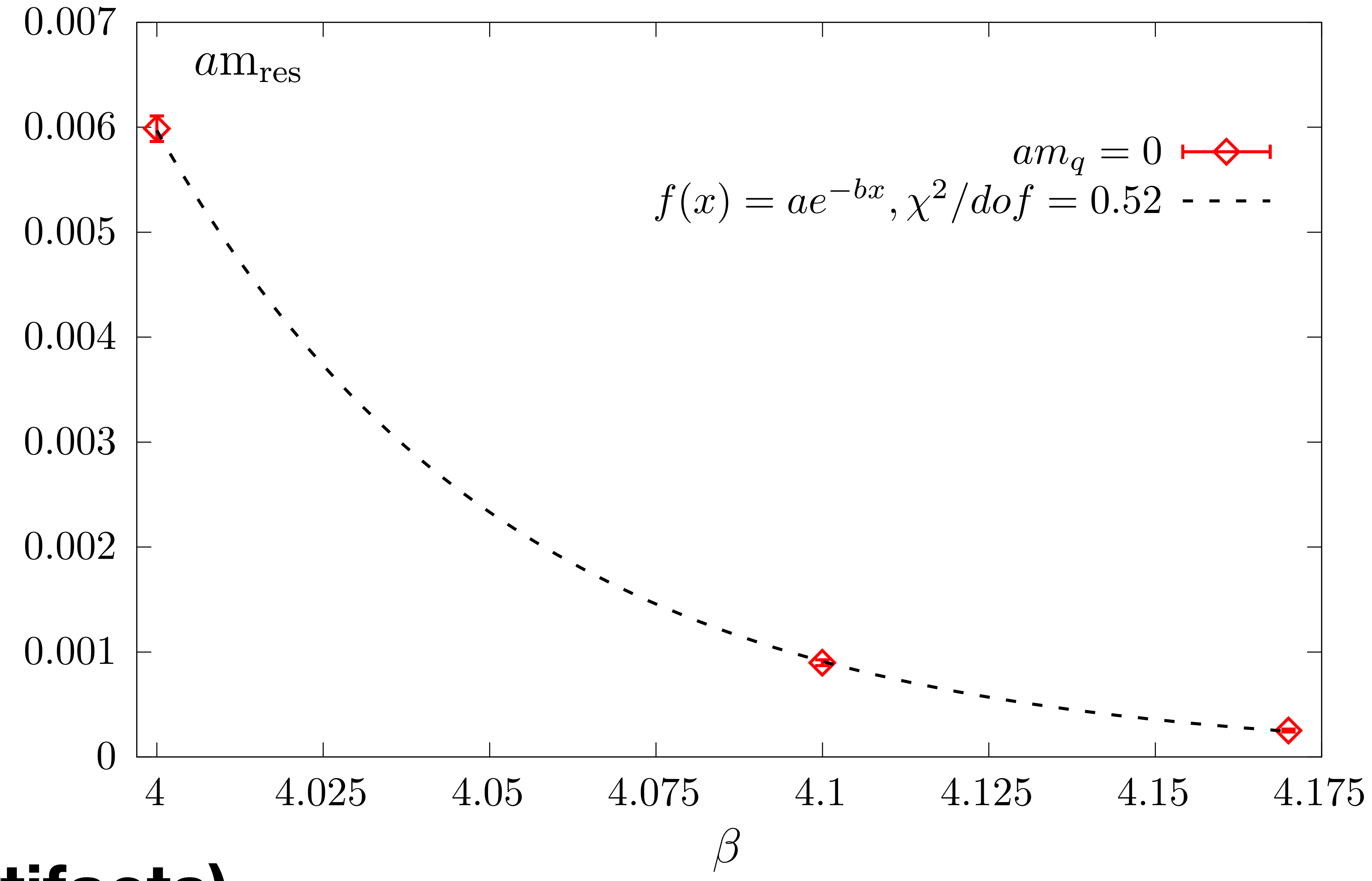

- m_{res} **has a linear dependence on** m_q **(lattice artifacts)**
  - **At** $am_q = 0$**:** $am_{\rm res} = 0.00613(9)$ **for** $L_s = 16$, $am_{\rm res} = 0.00324(3)$ **for** $L_s = 32$
- **At strong coupling,** m_{res} **dominated by gauge field dislocations, suppressed by** $1/L_s$
- **Coupling dependence:** m_{res} **increases exponentially as decrease** β

Pion mass

- **At leading order in chiral perturbation theory**
  $m_\pi^2 \propto m_q + m_{res}$

- **Evidence of good linearity**

- **m_π close to zero, but not exact**
zero at chiral limit:
  due to not considering chiral logarithm term & finite volume effects?

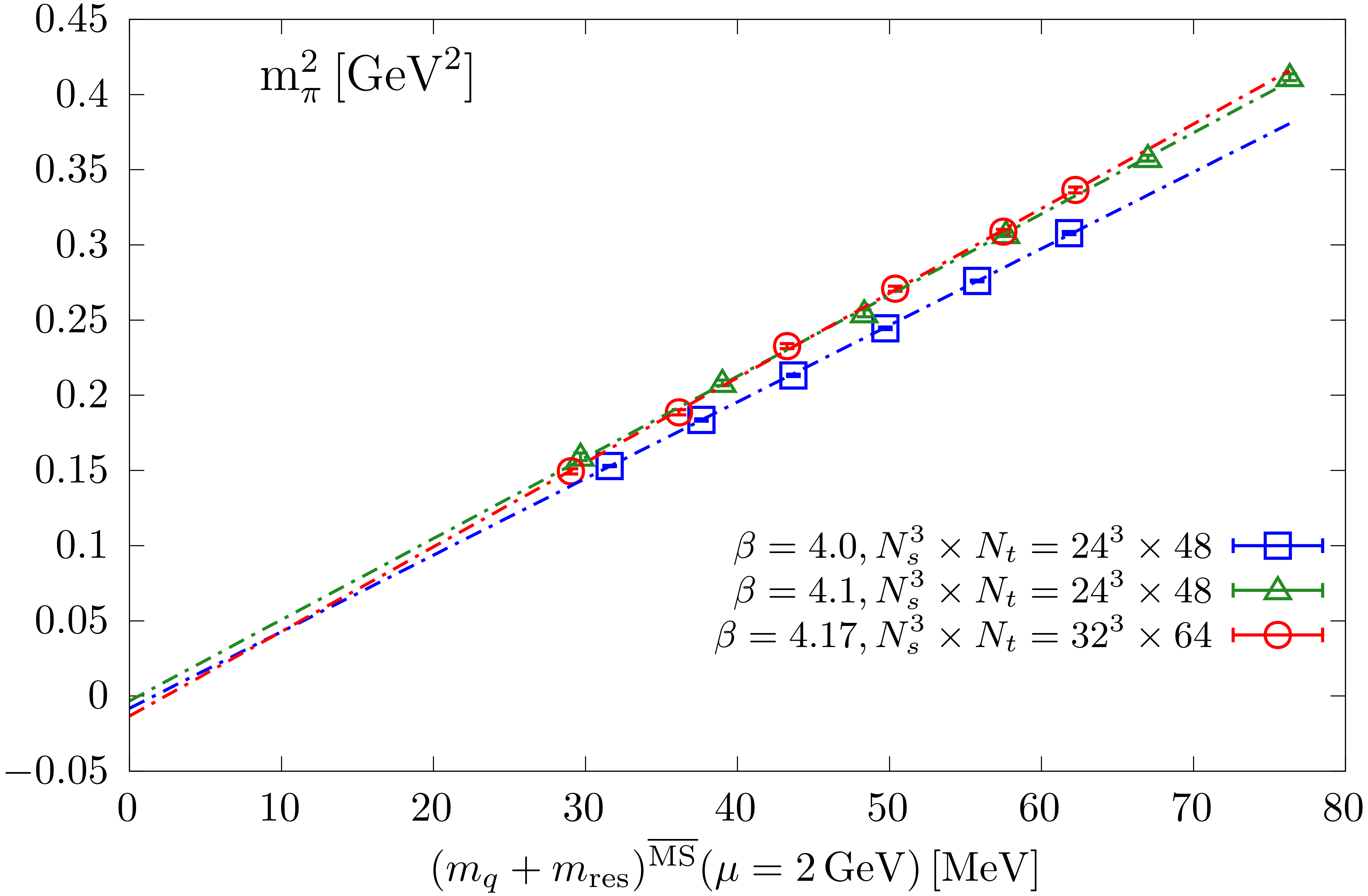

Good test of chirality

Chiral condensate

$$\langle\bar{\psi}\psi\rangle|_{\rm DWF} \sim \langle\bar{\psi}\psi\rangle|_{\rm cont.} + C^D \frac{m_q + x m_{res}}{a^2} + \ldots$$

[S. Sharpe, arXiv: 0706.0218]

- $x = \mathcal{O}(1)$ but $x \neq 1$
- Additive divergence remains by $m = m_q + m_{res} \to 0$:

$$\lim_{m\to 0}\lim_{L\to 0}\langle\bar{\psi}\psi\rangle|_{DWF} \sim \langle\bar{\psi}\psi\rangle|_{\rm cont.} + C^D \frac{(x-1)m_{res}}{a^2}$$

Two ways of subtracting divergences:

- $\langle\bar{\psi}\psi\rangle^{\rm ren} = Z_m^{-1}\left[\langle\bar{\psi}\psi\rangle^{\rm T>0} - \langle\bar{\psi}\psi\rangle^{\rm T=0}\right]$
- $\langle\bar{\psi}\psi\rangle^{\rm ren} = Z_m^{-1}\left[\langle\bar{\psi}\psi\rangle - C^D \frac{m_q + x m_{res}}{a^2}\right]$**, If we know C^D and x**

Zero T results

Calculate C^D for subtracting UV divergence term $C^D \frac{m_q + x m_{res}}{a^2}$

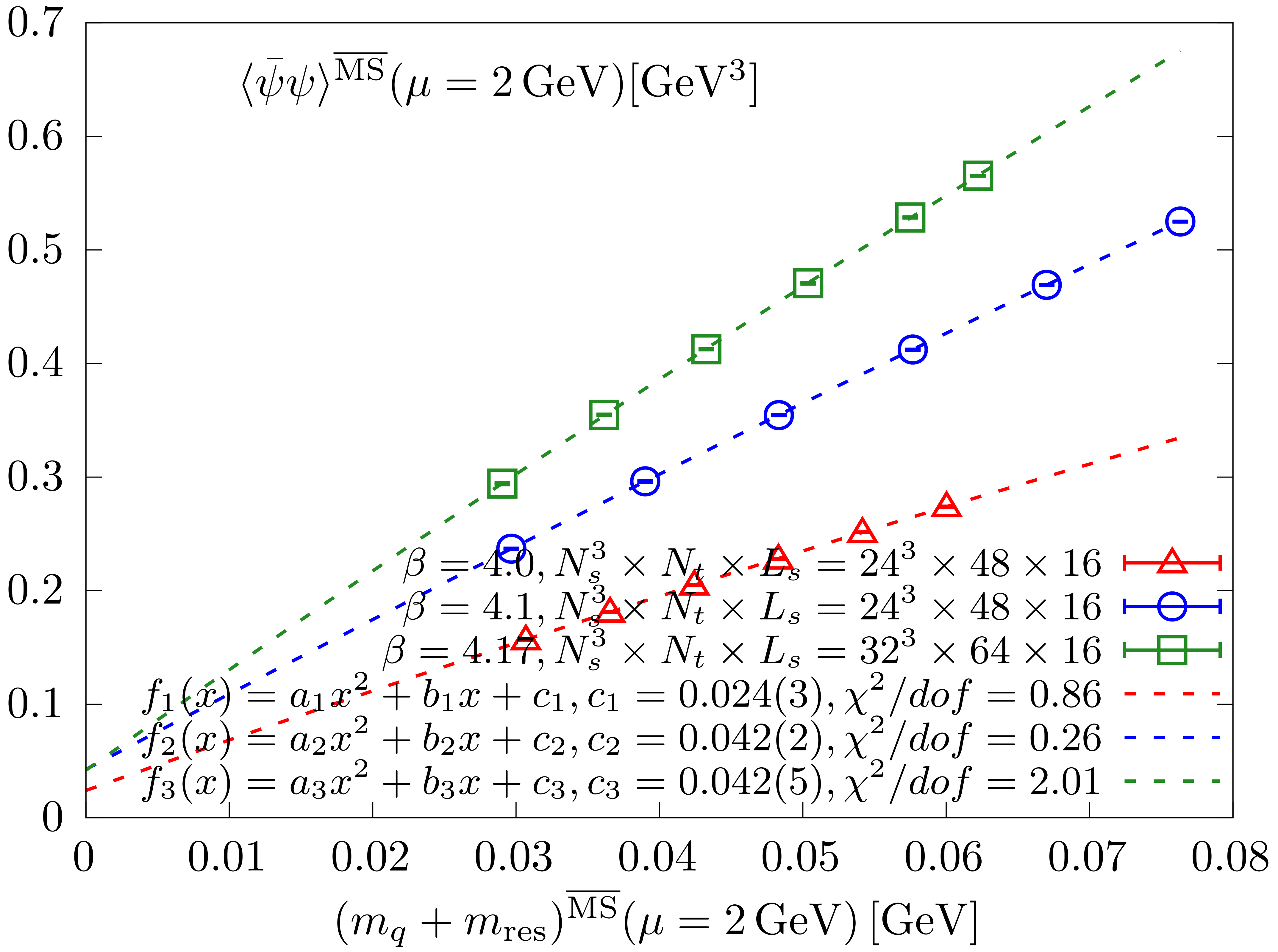

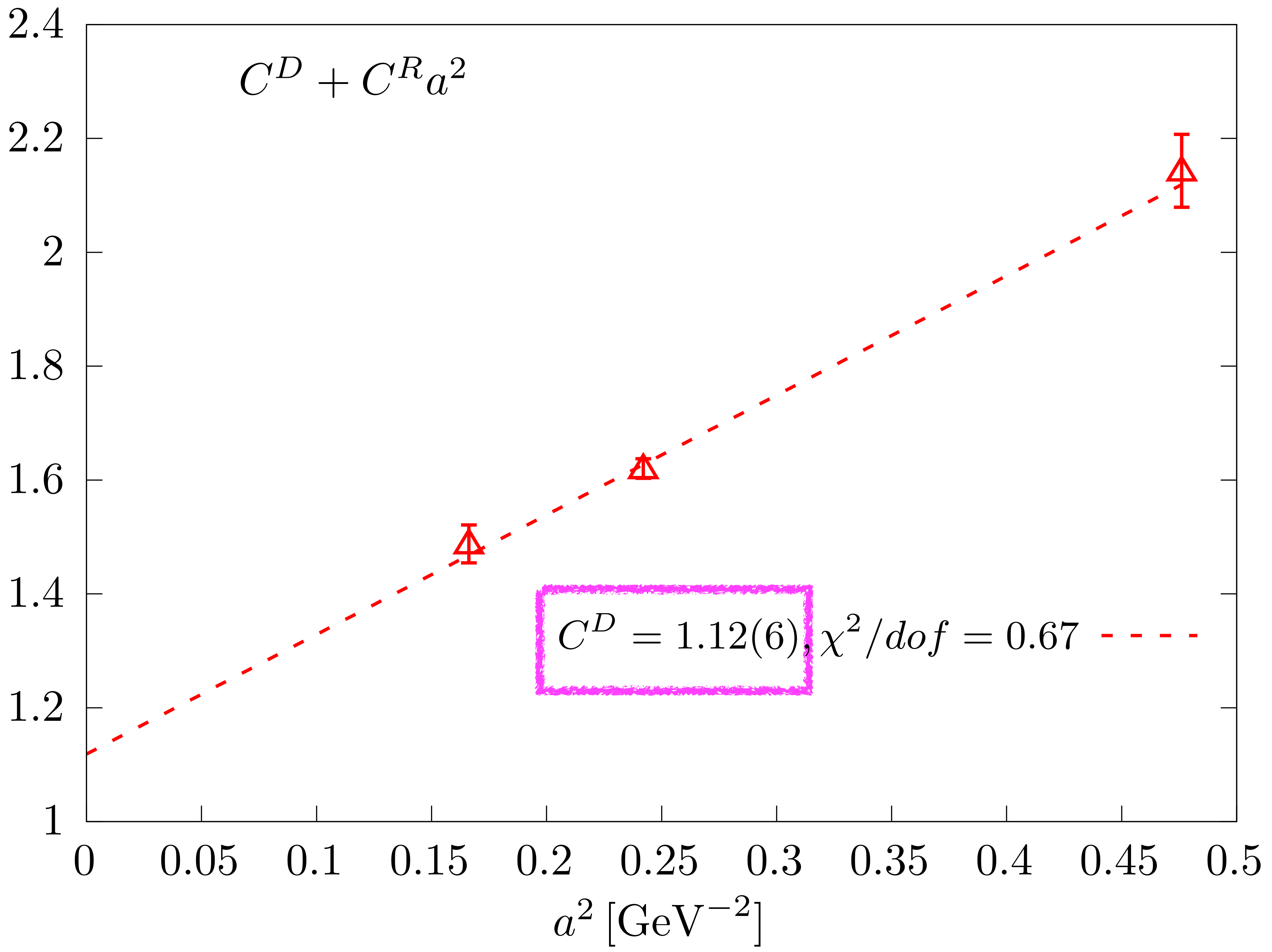

$$\langle\bar\psi\psi\rangle(m_q + m_{res}) = \langle\bar\psi\psi\rangle(0) + C^D\frac{m_q + x m_{res}}{a^2} + C^R(m_q + m_{res}) + A(m_q + m_{res})^2$$

$$= \langle\bar\psi\psi\rangle(0) + (C^D + C^R a^2)\frac{m_q + m_{res}}{a^2} + C^D\frac{(x-1)m_{res}}{a^2} + A(m_q + m_{res})^2$$

Finite T results

Calculate x for subtracting UV divergence term $C^D \frac{m_q + x m_{res}}{a^2}$

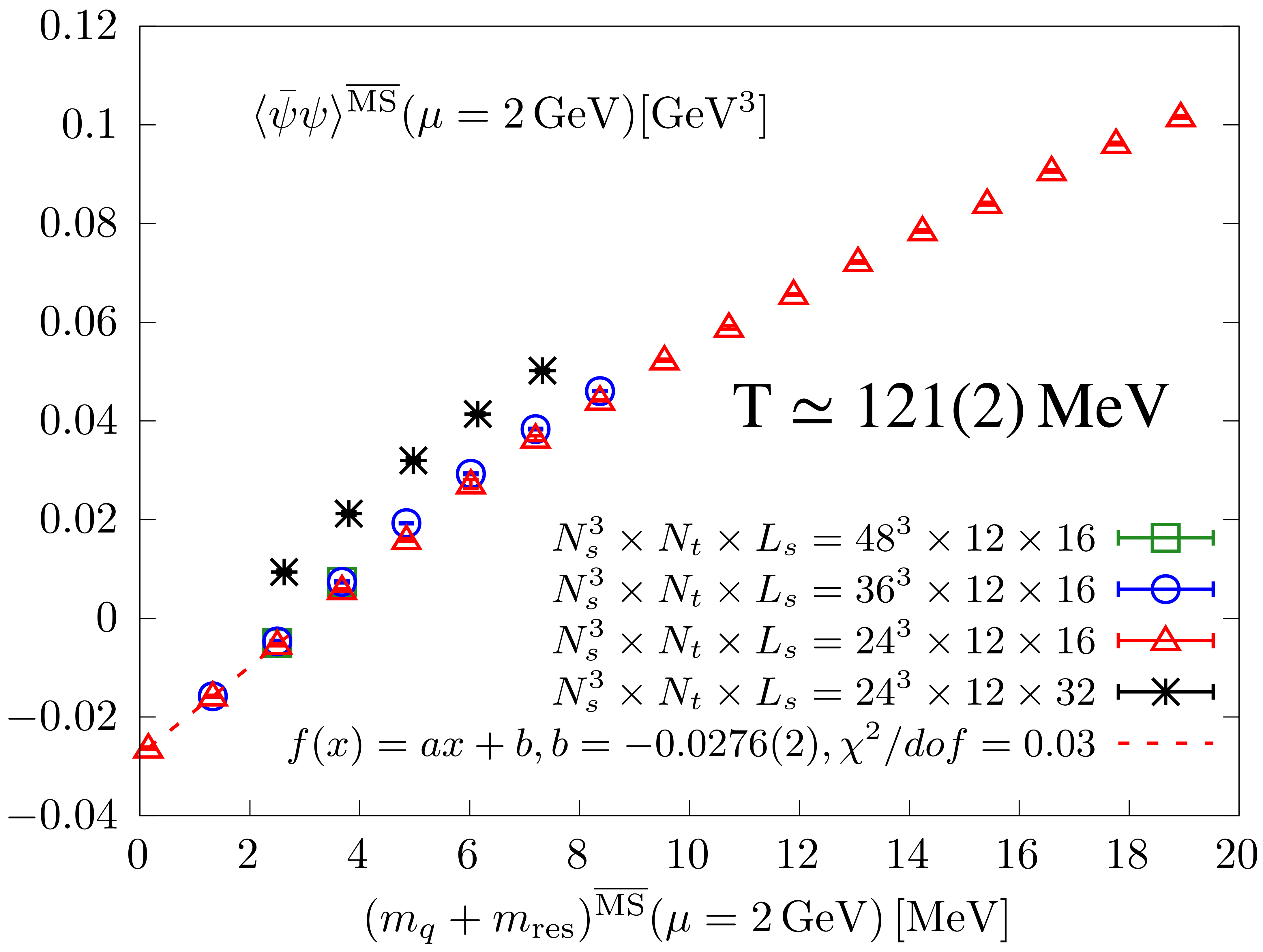

$$\lim_{(m_q+m_{res})\to 0} \langle\bar\psi\psi\rangle|_{DWF} \sim \langle\bar\psi\psi\rangle|_{cont.} + C^D \frac{(x-1)m_{res}}{a^2}$$

$$T_c = 98^{+3}_{-6}\,\text{MeV}$$

$x = -0.6(1)$ **for T>T$_c$**

[S. Sharma et al. PRD 2022]

Renormalized chiral condensate

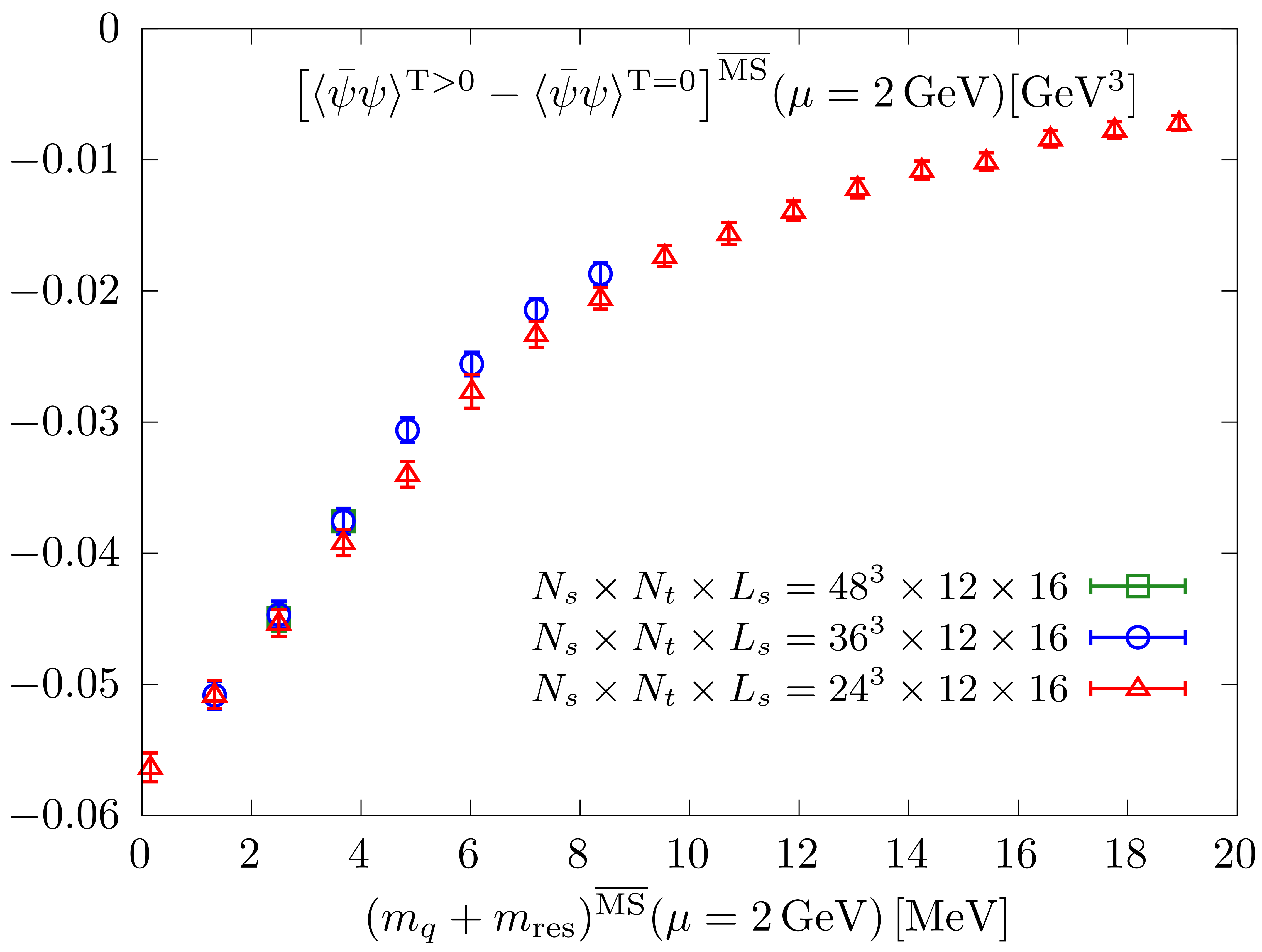

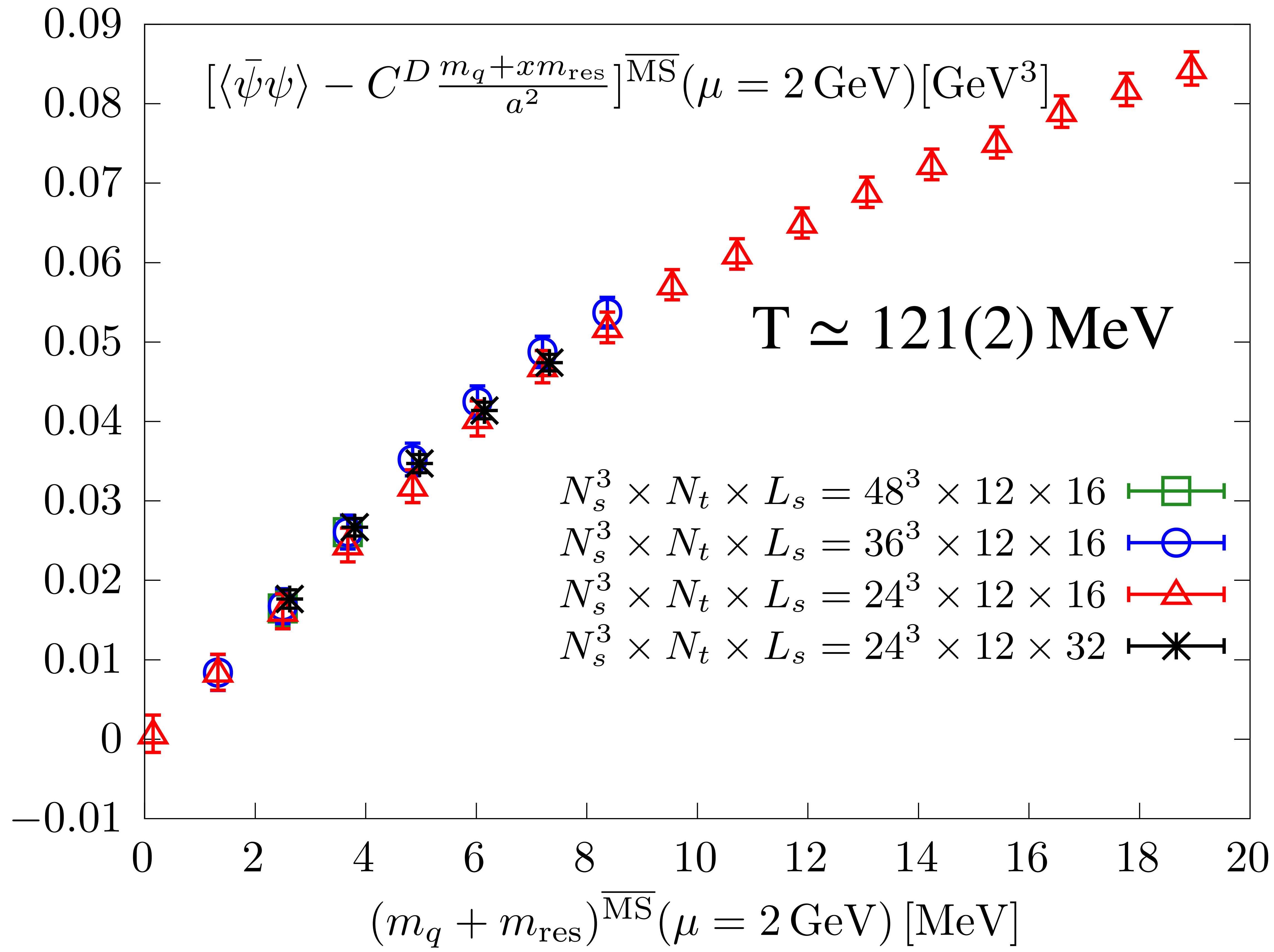

- **Subtracted chiral condensate vanishes in the chiral limit**
- **Finite volume effect is visible at low T**
- **Subtracted chiral condensate remains the same with same total quark mass for varying Ls**

Renormalized chiral condensate

Multiplicatively renormalized chiral condensate

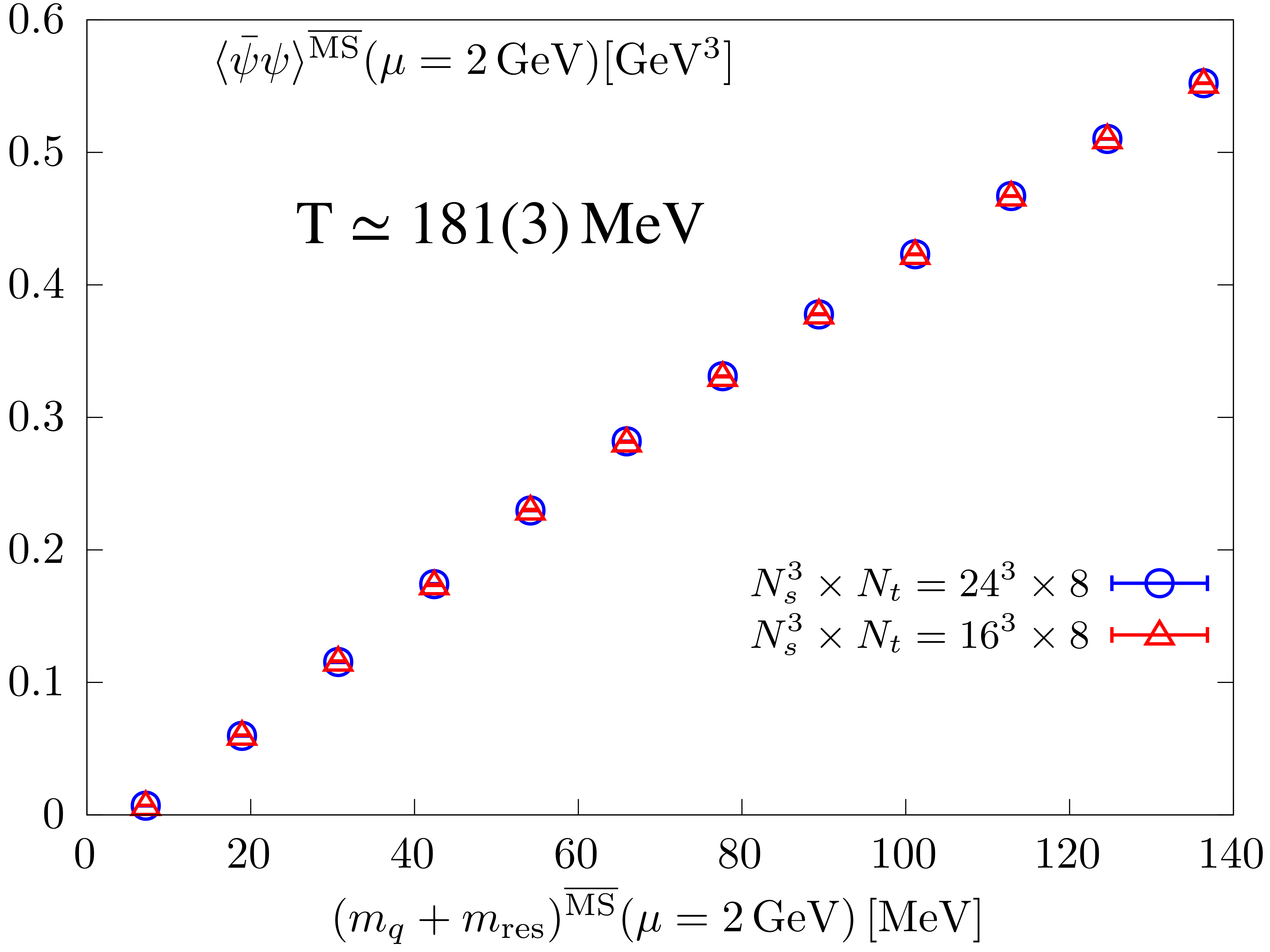

Additive and multiplicatively renormalized chiral condensate

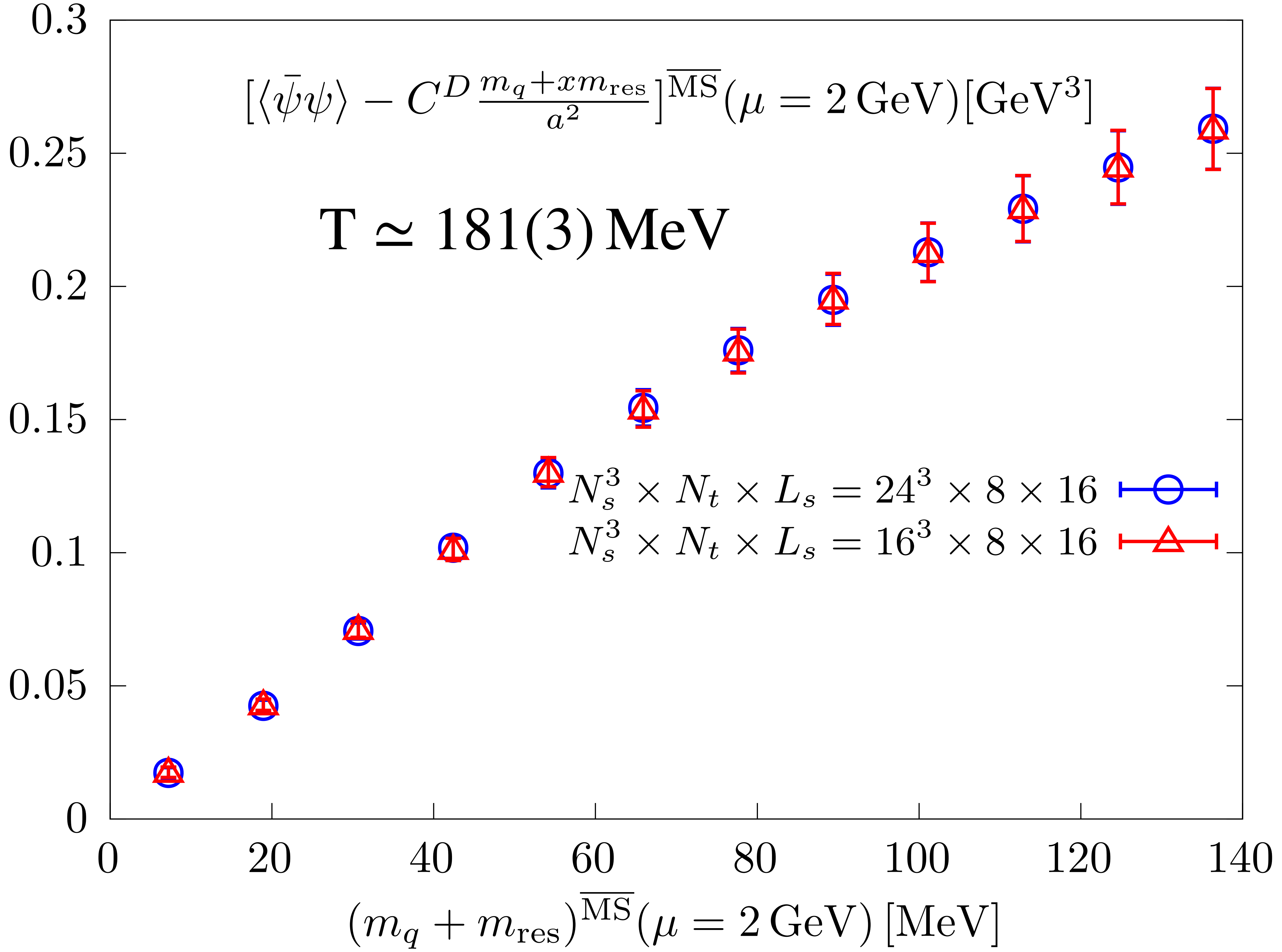

Subtracted chiral condensate vanishes in the chiral limit as expected since T> T_c

Disconnected chiral susceptibility

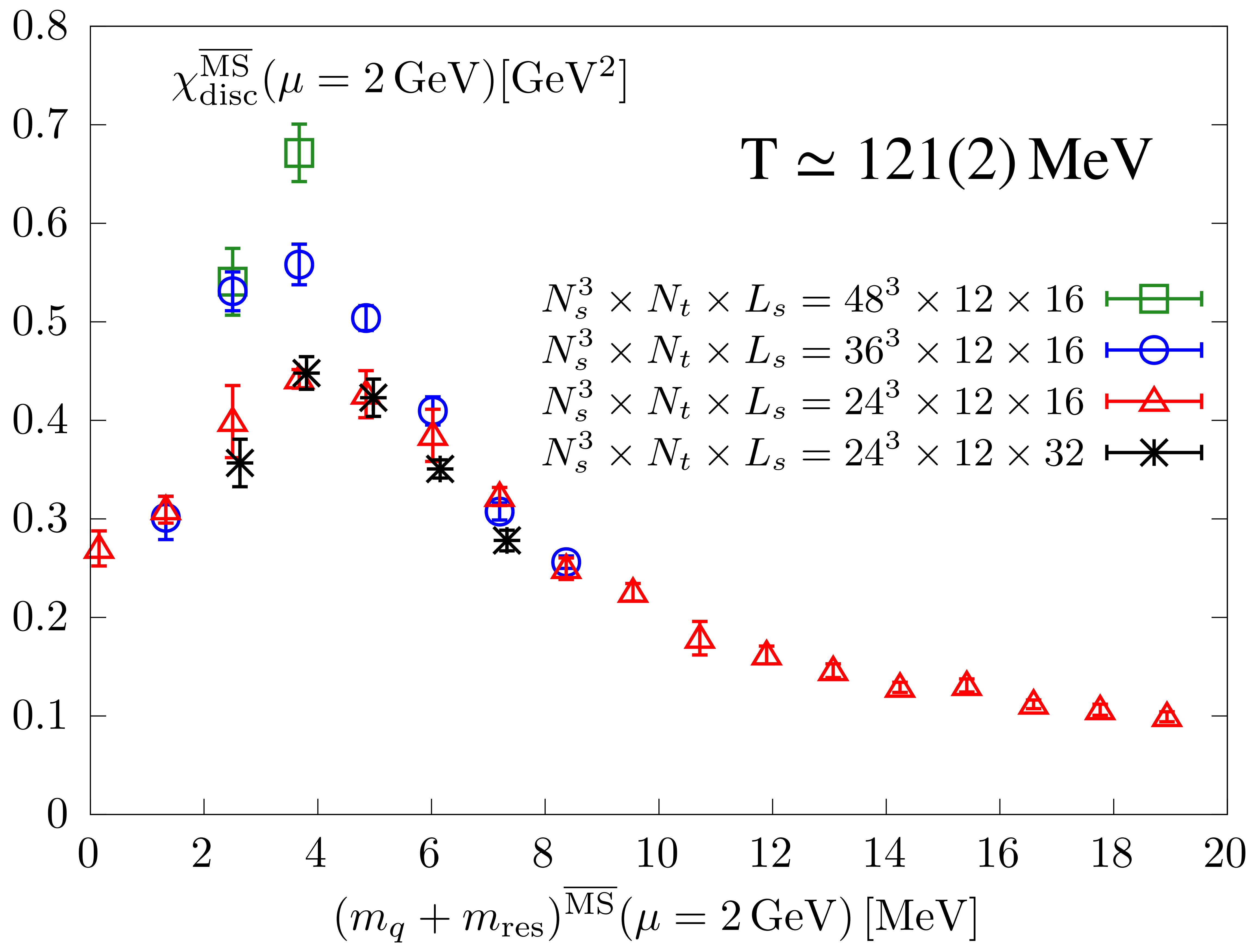

- **Large finite volume effect near the transition point, but the change in peak height is not as large as anticipated from a real phase transition**

  ➡ **Consistent with the crossover transition**

- **The transition mass point is around 3.6 MeV**

  (FLAG Review '21: $m_{ud}^{\overline{\rm MS}}(2\,{\rm GeV}) = 3.381(40)\,{\rm MeV}$)

- χ_{disc} **seems to be function of total quark mass**

Finite size scaling: susceptibility

- Crossover: $\chi_{tot}^{\max}(N_s, N_t)$ independent of V
- 1st order PT: $\chi_{tot}^{\max}(N_s, N_t) \propto V$
- Z(2) 2nd order PT: a singular behavior should be observed in $\chi_{tot}^{\max}(N_s, N_t)$ with V $((N_s^3 \times N_t)^\alpha,\ \alpha = 1.966$ is the critical exponent)

The peak height of χ_{tot} does not scale like a 1st or Z(2) second order PT

finite-size scaled renormalized chiral susceptibility

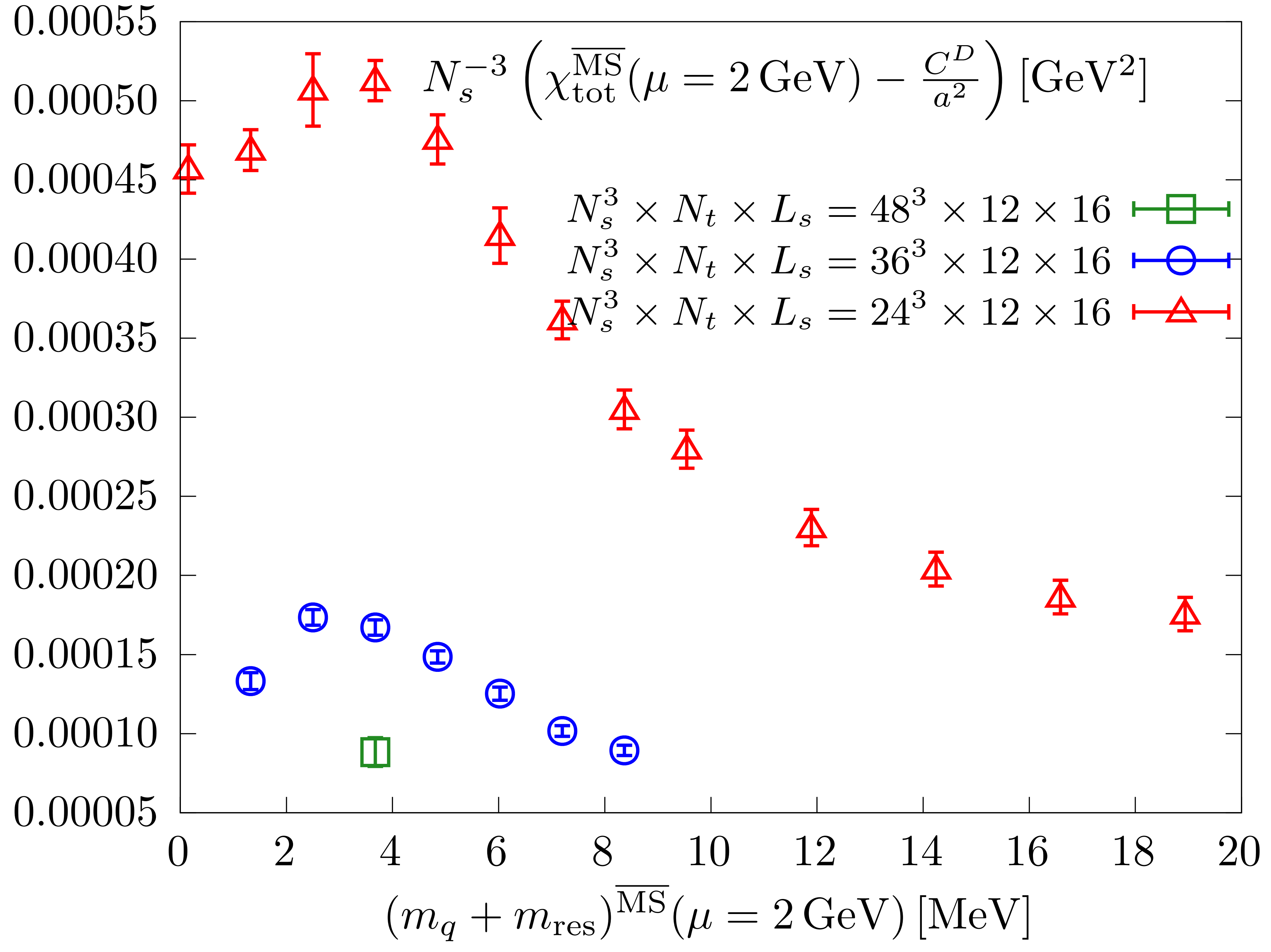

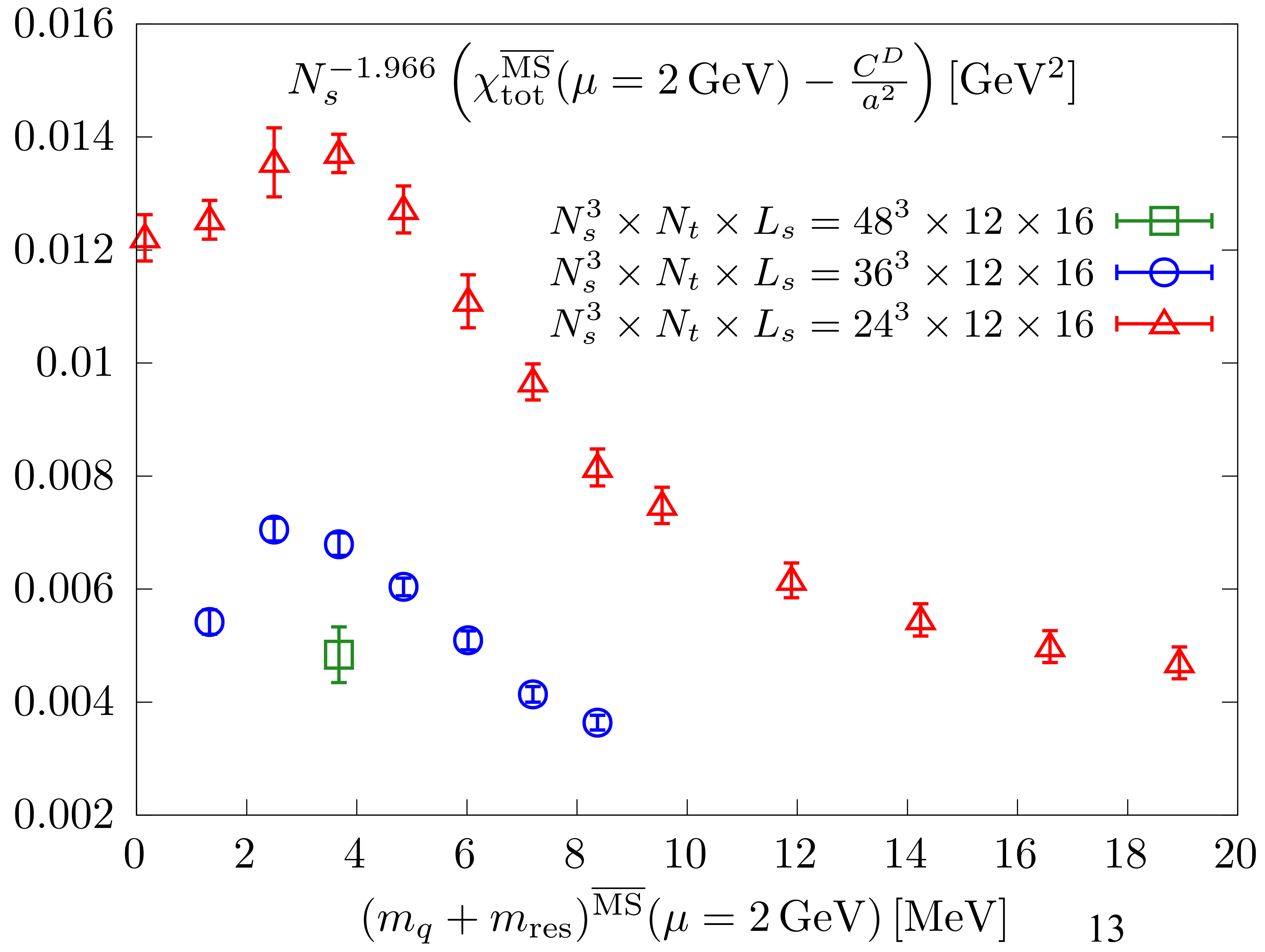

Binder Cumulant

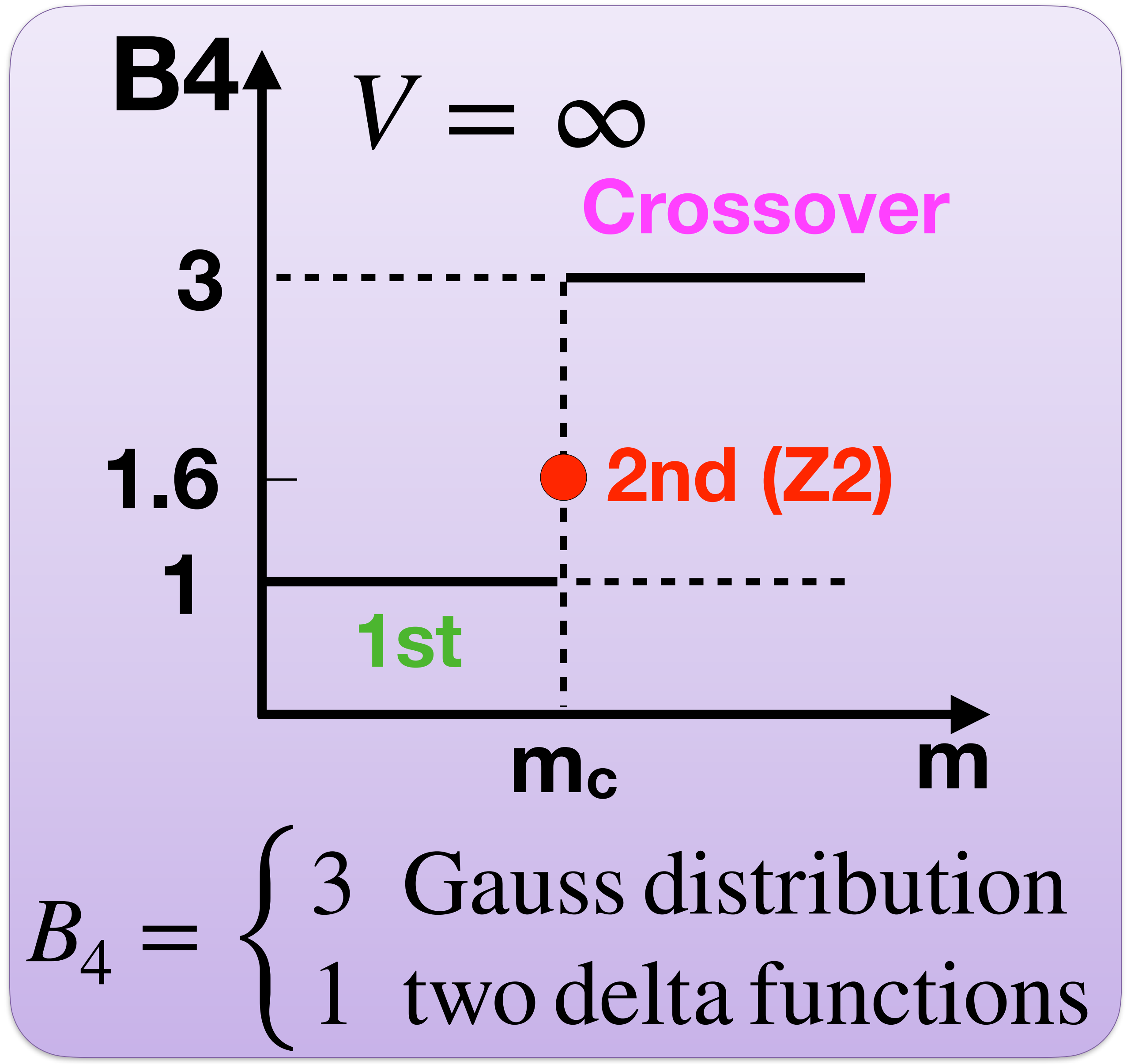

A.Kiyohara et al., PRD 104, 114509 (2021)

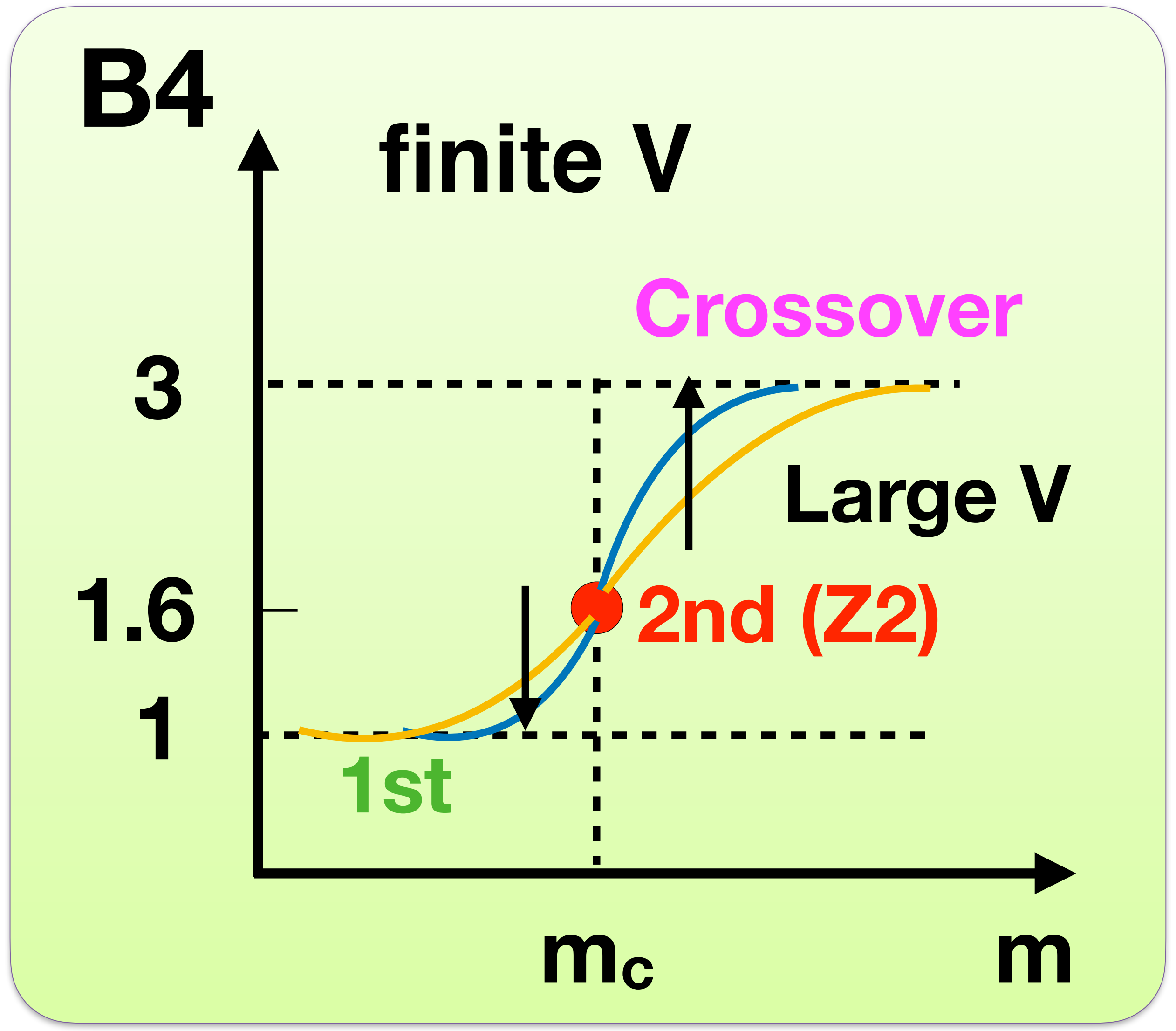

$$B_4(\bar{\psi}\psi) = \frac{\langle(\delta\bar{\psi}\psi)^4\rangle}{\langle(\delta\bar{\psi}\psi)^2\rangle^2}, \quad \delta\bar{\psi}\psi = \bar{\psi}\psi - \langle\bar{\psi}\psi\rangle$$

Suggests a crossover transition at $(m_q + m_{\rm res})^{\overline{\rm MS}}(2\,{\rm GeV}) \simeq$ **3.6 MeV**

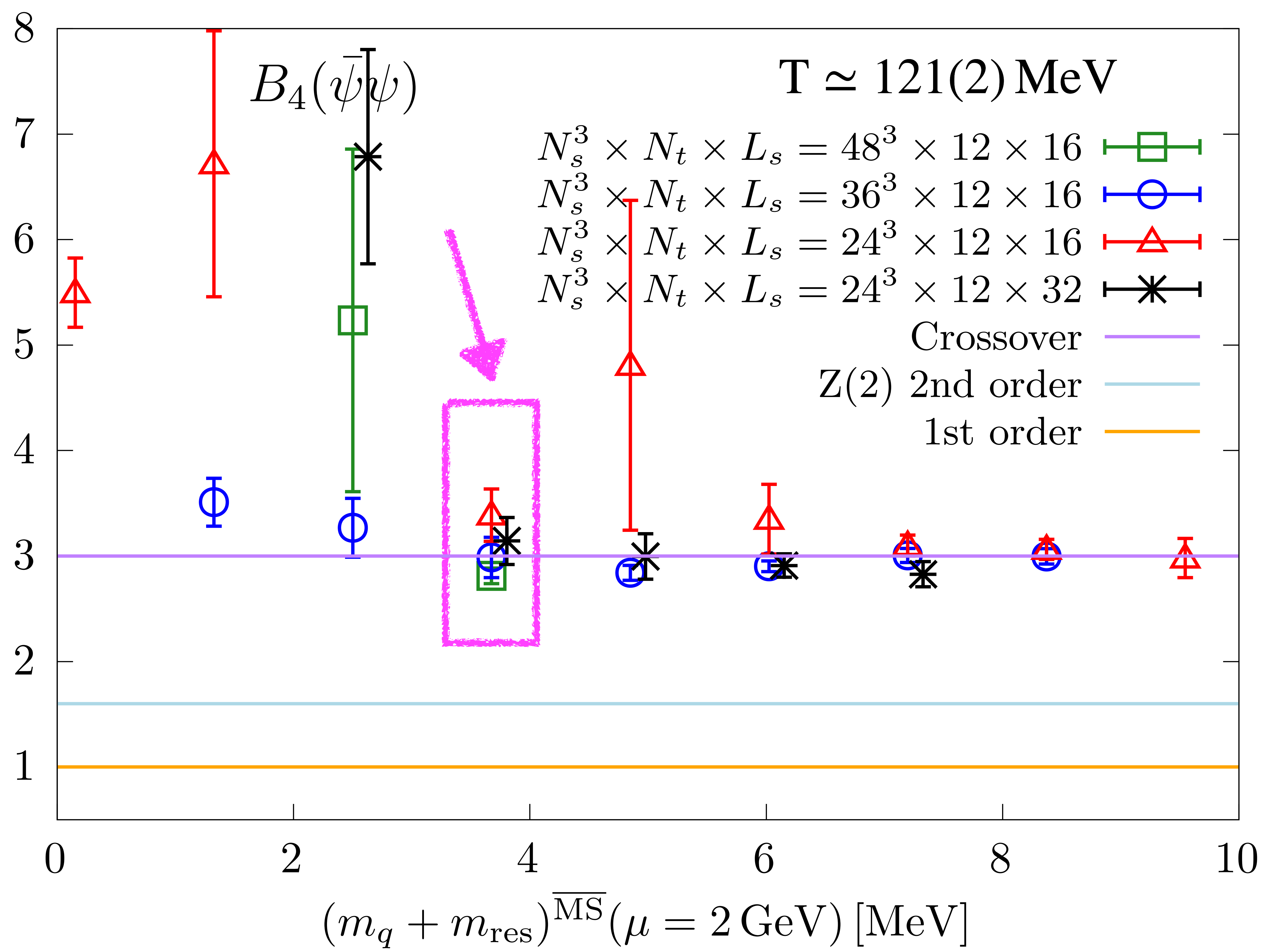

Histogram of chiral condensate near transition point

Behaves like a Gaussian distribution, no evidence of a double peak structure would appear as $V \uparrow$

Summary and outlook

No evidence of a 1st order PT in our explored quark mass range
If a 1st order region exist, the critical mass should be less than 3.6 MeV

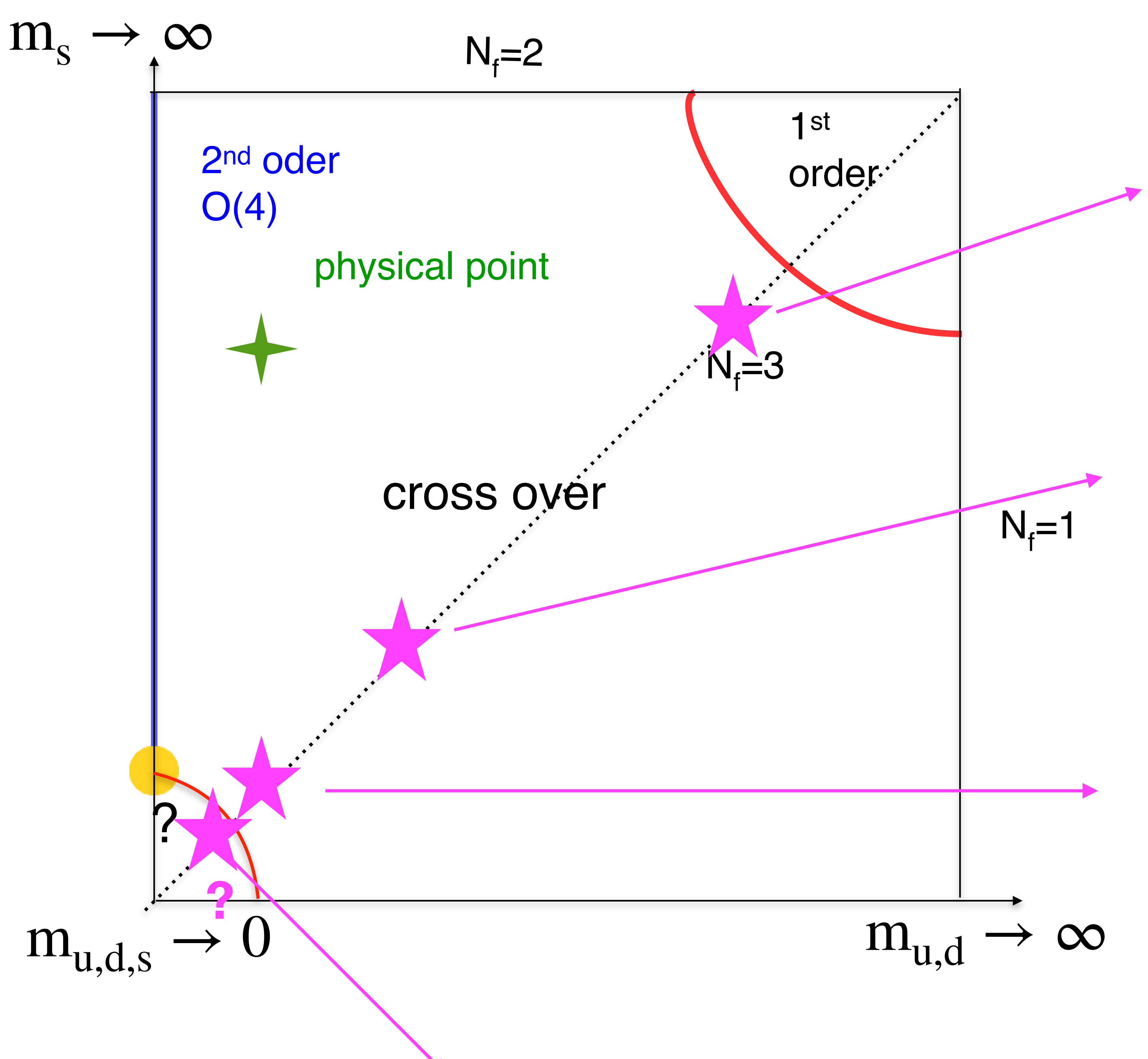

- $T \sim 242\,\text{MeV}(N_t = 6), (m_q + m_{\text{res}})^{\overline{\text{MS}}}_{pc} \sim 183\,\text{MeV}$
  $\Leftrightarrow m_\pi^{pc} \sim 997\,\text{MeV}$, crossover transition

  Y. Nakamura, Y. Zhang et al., *PoS* LATTICE2021

- $T \sim 181\,\text{MeV}(N_t = 8), (m_q + m_{\text{res}})^{\overline{\text{MS}}}_{pc} \sim 42\,\text{MeV}$
  $\Leftrightarrow m_\pi^{pc} \sim 476\,\text{MeV}$, crossover transition

  Y. Zhang et al., *PoS* LATTICE2022

- $T \sim 121\,\text{MeV}(N_t = 12), (m_q + m_{\text{res}})^{\overline{\text{MS}}}_{pc} \sim 3.6\,\text{MeV}$
  $\Leftrightarrow m_\pi^{pc} \sim 141\,\text{MeV}$, crossover transition

  Y. Zhang et al., *PoS* LATTICE2023

- $T \sim 104\,\text{MeV}\,(N_t = 14)$, lighter quark mass simulation is underway

Acknowledgements

- Codes
  - HMC
    - Grid (implementation for A64FX: thanks to the Regensburg group)
  - Measurements
    - Bridge++
    - Hadrons / Grid

- Computers
  - Supercomputer Fugaku provided by the RIKEN Center for Computational Science through HPCI project #hp210032 and Usability Research ra000001.
  - Wisteria/BDEC-01 Oddysey at Univ. Tokyo/JCAHPC through HPCI project #hp220108 Ito supercomputer at Kyushu University through HPCI project #hp190124 and hp200050
  - Hokusai BigWaterfall at RIKEN

- Grants
  - JSPS Kakenhi (20H01907)

Backup slide

Chiral susceptibility

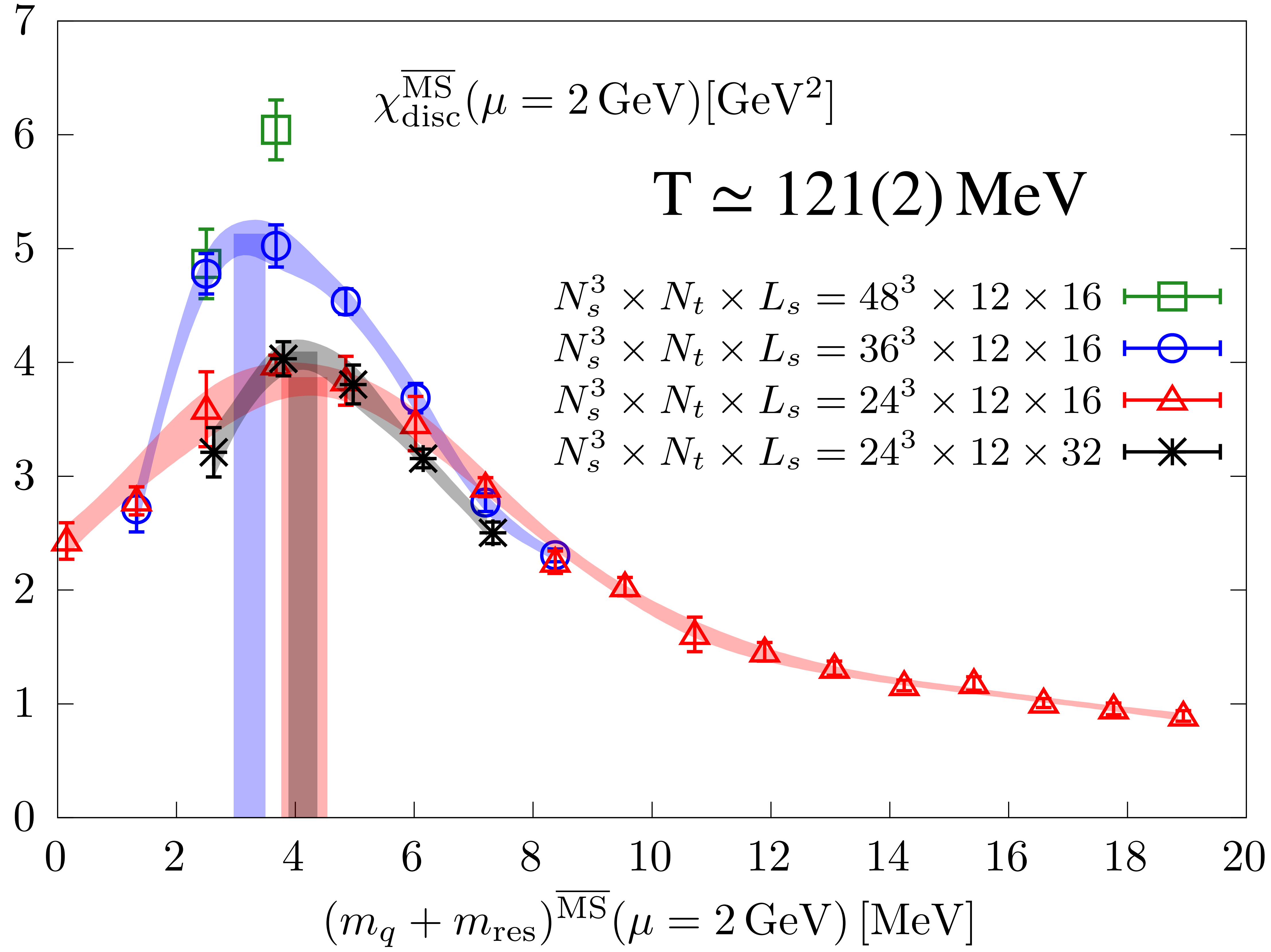

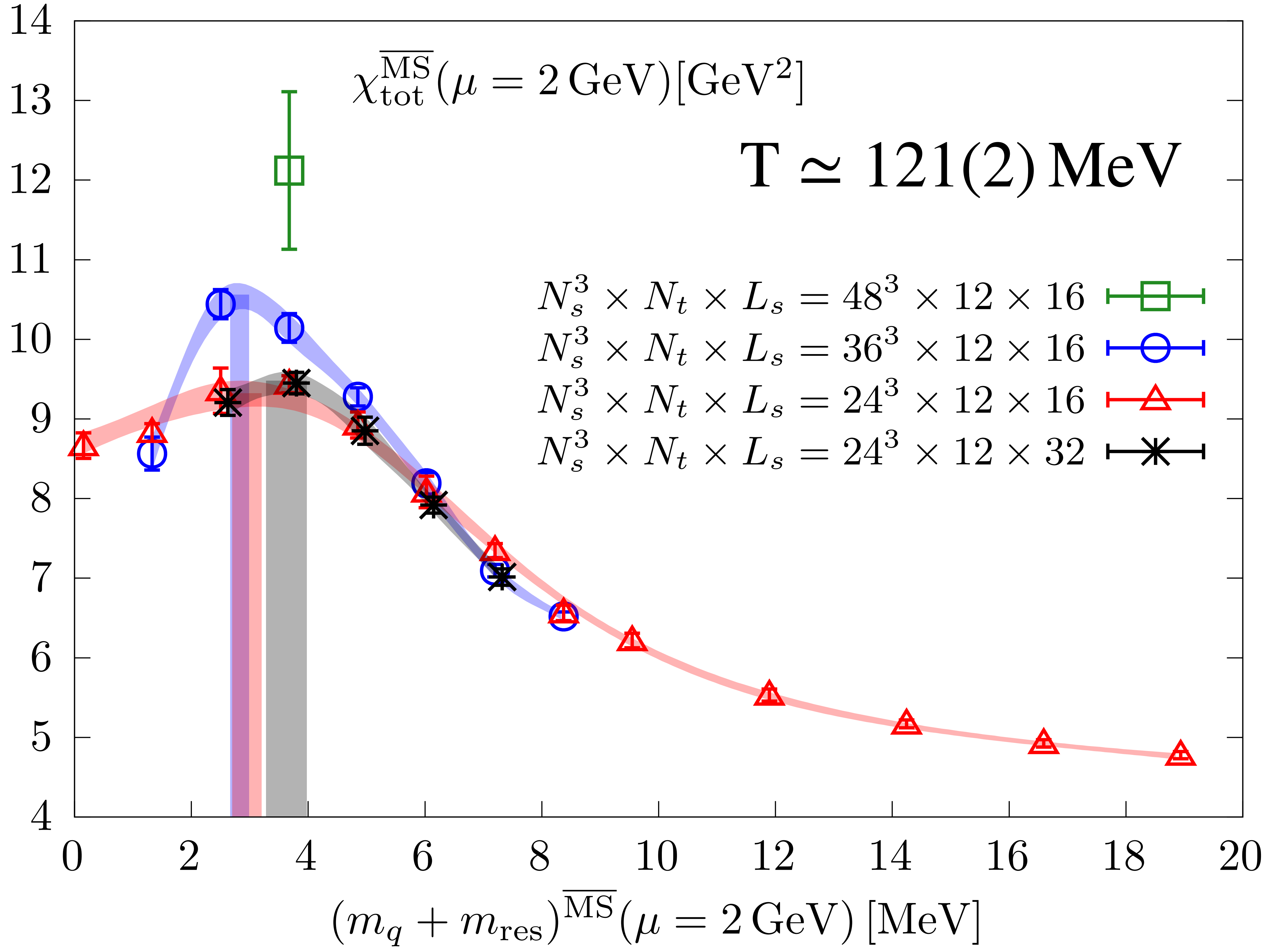

- **Large finite volume effect near the transition point, but the change in peak height is not as large as anticipated from a real phase transition ➡ Consistent with the crossover transition**
- **The transition mass point is around 2.7-4.5 MeV** (FLAG Review '21: $m_{ud}^{\overline{\rm MS}}(2\,{\rm GeV}) = 3.381(40)\,{\rm MeV}$)
- **Chiral susceptibilities seem to be function of total quark mass**

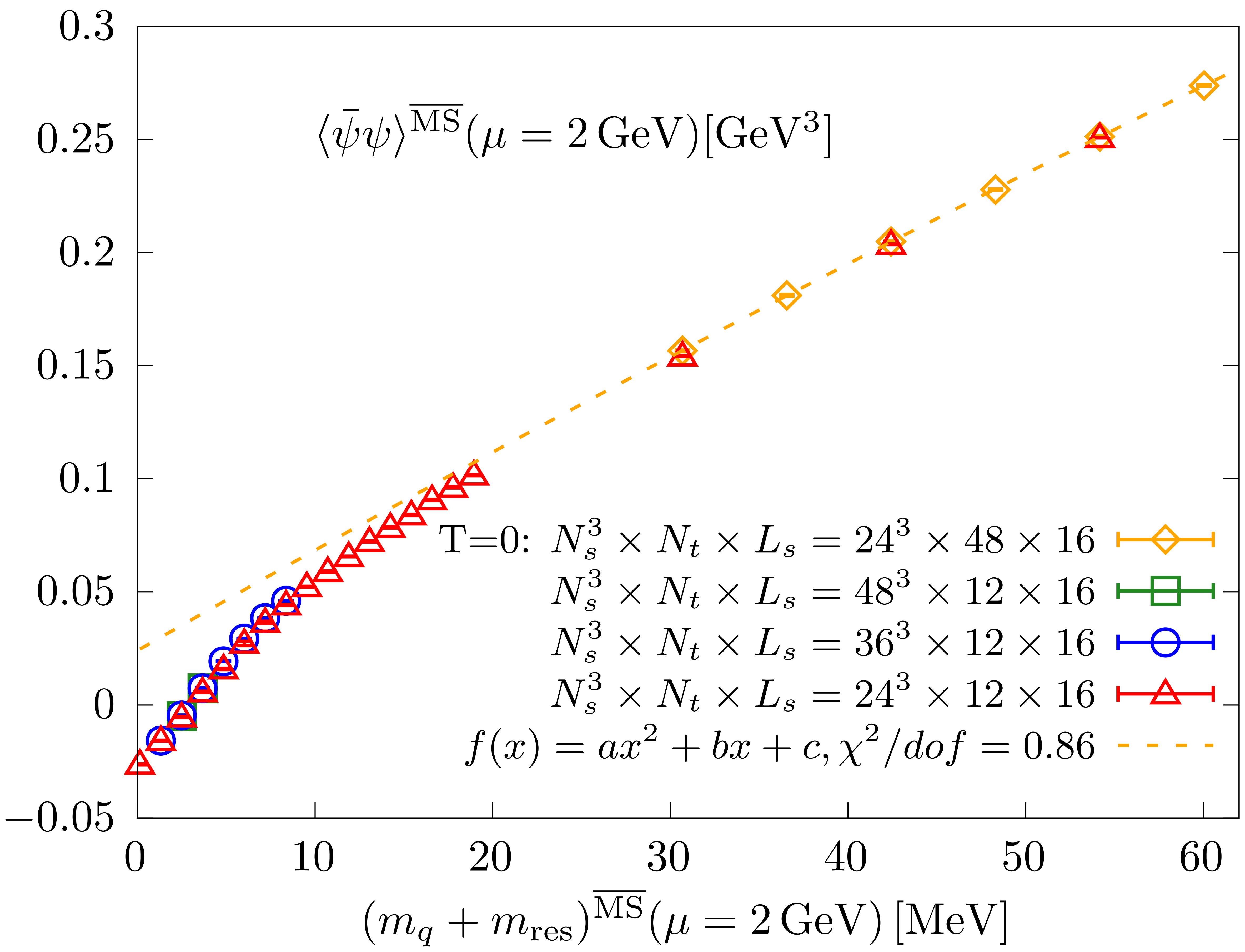

$\langle\bar{\psi}\psi\rangle^{\overline{\rm MS}}(\mu = 2\,{\rm GeV})[{\rm GeV}^3]$
0.3
0.25
0.2
0.15
0.1
0.05
0
−0.05
0
10
20
30
40
50
60
$(m_q + m_{\rm res})^{\overline{\rm MS}}(\mu = 2\,{\rm GeV})$ [MeV]
T=0: $N_s^3 \times N_t \times L_s = 24^3 \times 48 \times 16$
$N_s^3 \times N_t \times L_s = 48^3 \times 12 \times 16$
$N_s^3 \times N_t \times L_s = 36^3 \times 12 \times 16$
$N_s^3 \times N_t \times L_s = 24^3 \times 12 \times 16$
$f(x) = ax^2 + bx + c, \chi^2/dof = 0.86$

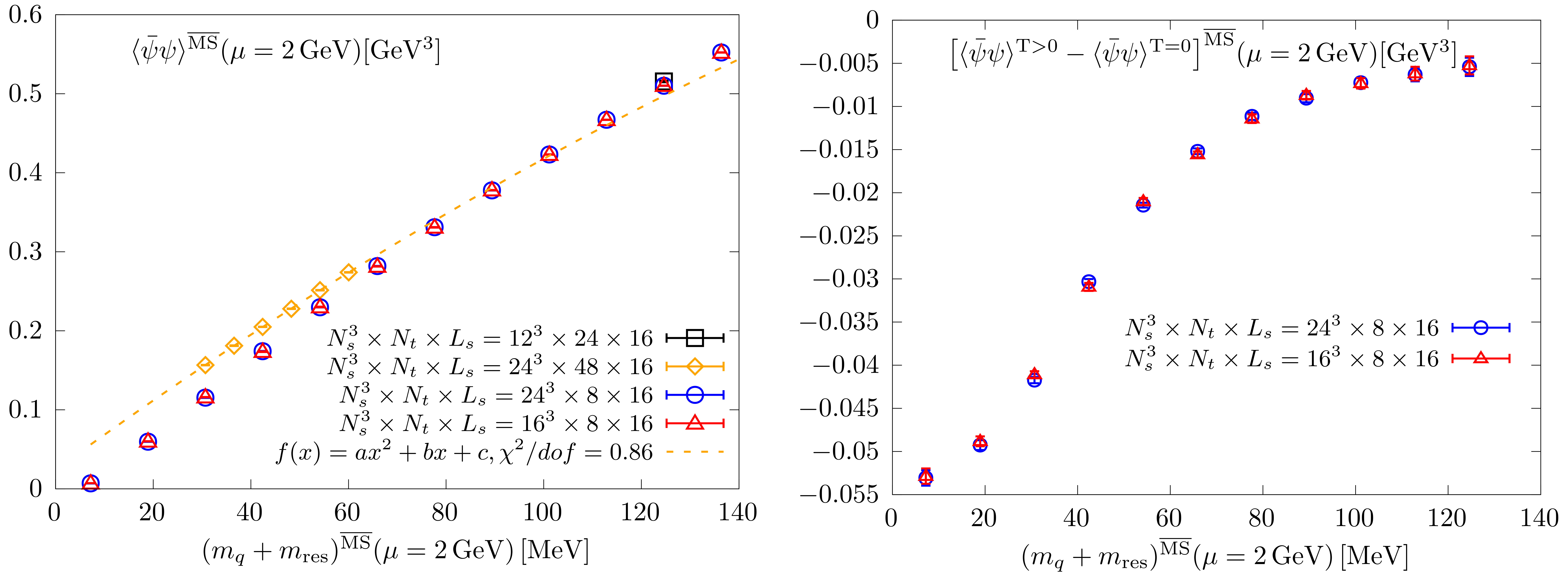

$\langle\bar{\psi}\psi\rangle^{\overline{\rm MS}}(\mu = 2\,{\rm GeV})[{\rm GeV}^3]$
$N_s^3 \times N_t \times L_s = 12^3 \times 24 \times 16$
$N_s^3 \times N_t \times L_s = 24^3 \times 48 \times 16$
$N_s^3 \times N_t \times L_s = 24^3 \times 8 \times 16$
$N_s^3 \times N_t \times L_s = 16^3 \times 8 \times 16$
$f(x) = ax^2 + bx + c, \chi^2/dof = 0.86$
$(m_q + m_{\rm res})^{\overline{\rm MS}}(\mu = 2\,{\rm GeV})$ [MeV]
$[\langle\bar{\psi}\psi\rangle^{\rm T>0} - \langle\bar{\psi}\psi\rangle^{\rm T=0}]^{\overline{\rm MS}}(\mu = 2\,{\rm GeV})[{\rm GeV}^3]$
$N_s^3 \times N_t \times L_s = 24^3 \times 8 \times 16$
$N_s^3 \times N_t \times L_s = 16^3 \times 8 \times 16$
$(m_q + m_{\rm res})^{\overline{\rm MS}}(\mu = 2\,{\rm GeV})$ [MeV]

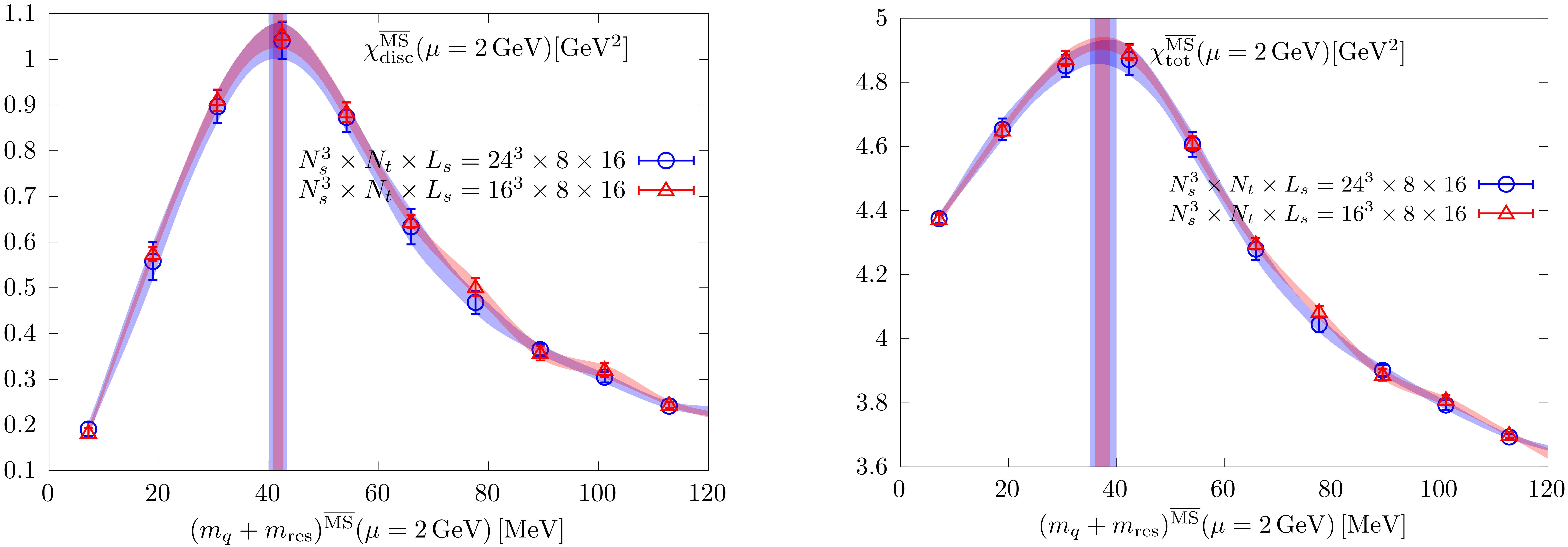

$\chi_{\rm disc}^{\overline{\rm MS}}(\mu = 2\,{\rm GeV})[{\rm GeV}^2]$
$N_s^3 \times N_t \times L_s = 24^3 \times 8 \times 16$
$N_s^3 \times N_t \times L_s = 16^3 \times 8 \times 16$
$(m_q + m_{\rm res})^{\overline{\rm MS}}(\mu = 2\,{\rm GeV})$ [MeV]
$\chi_{\rm tot}^{\overline{\rm MS}}(\mu = 2\,{\rm GeV})[{\rm GeV}^2]$
$N_s^3 \times N_t \times L_s = 24^3 \times 8 \times 16$
$N_s^3 \times N_t \times L_s = 16^3 \times 8 \times 16$
$(m_q + m_{\rm res})^{\overline{\rm MS}}(\mu = 2\,{\rm GeV})$ [MeV]

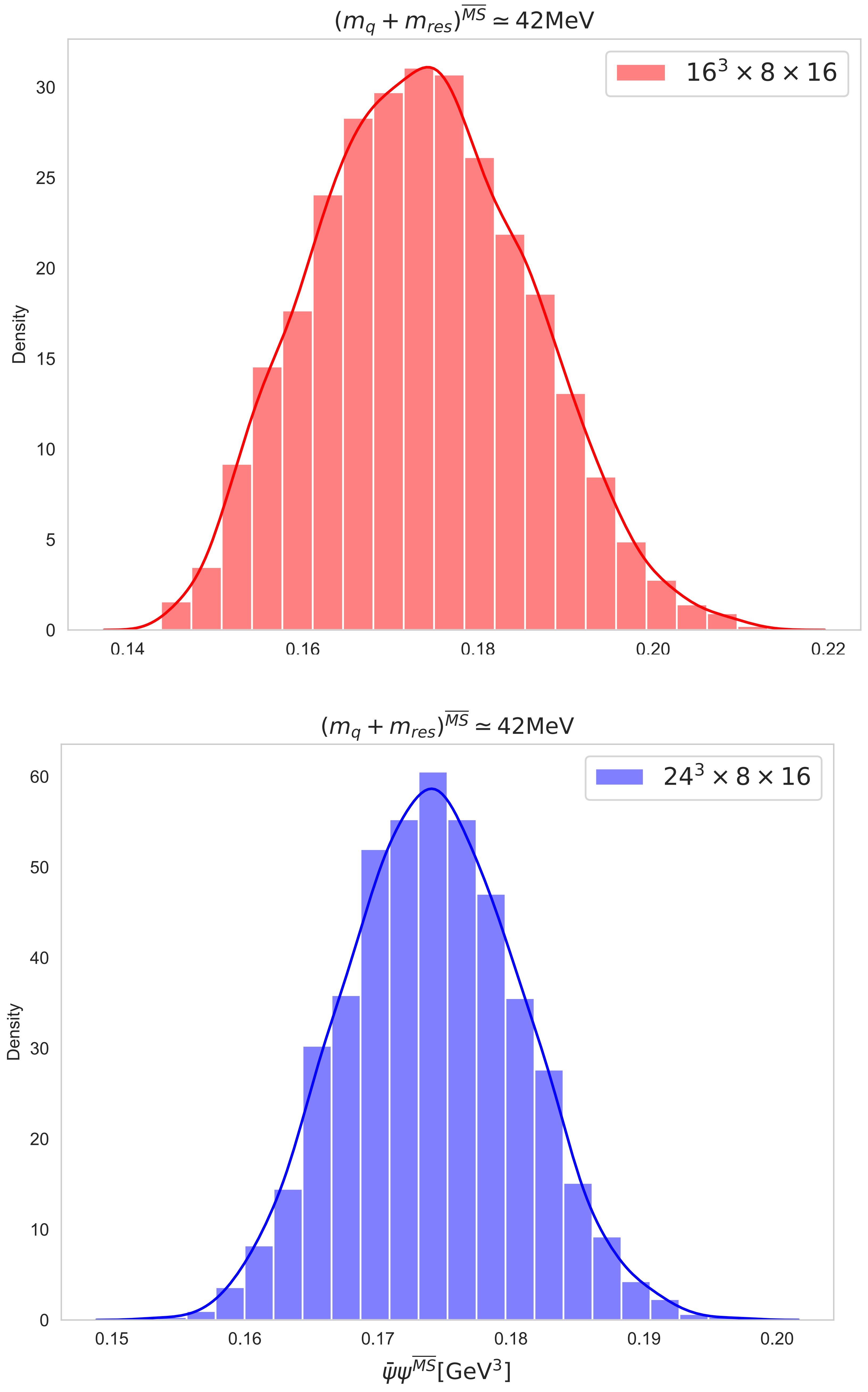

$(m_q + m_{res})^{\overline{MS}} \simeq 42$MeV
$16^3 \times 8 \times 16$
Density
$(m_q + m_{res})^{\overline{MS}} \simeq 42$MeV
$24^3 \times 8 \times 16$
Density
$\bar{\psi}\psi^{\overline{MS}}$[GeV^3]

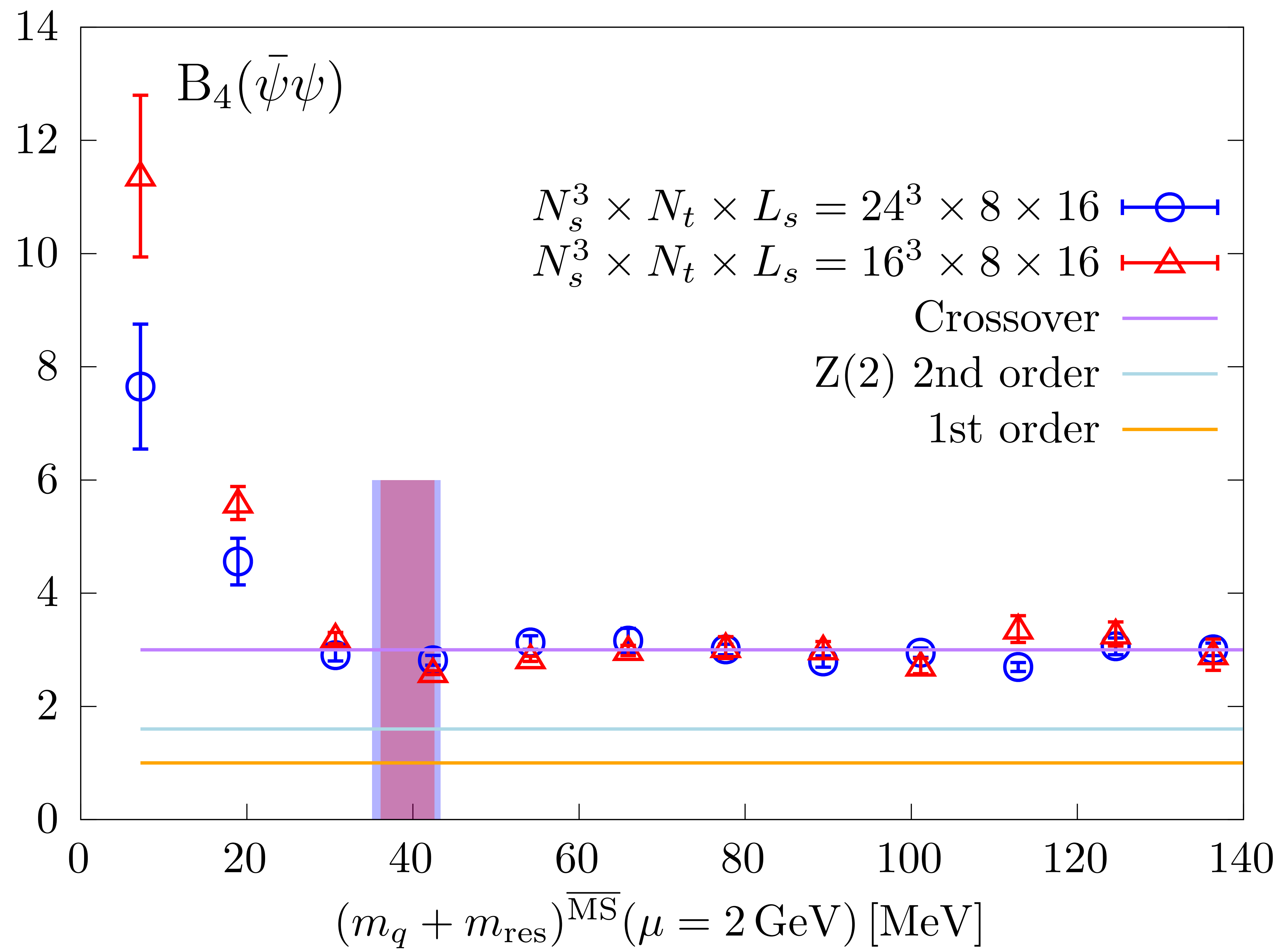

$B_4(\bar{\psi}\psi)$
$N_s^3 \times N_t \times L_s = 24^3 \times 8 \times 16$
$N_s^3 \times N_t \times L_s = 16^3 \times 8 \times 16$
Crossover
Z(2) 2nd order
1st order
$(m_q + m_{\rm res})^{\overline{\rm MS}}(\mu = 2\,{\rm GeV})$ [MeV]

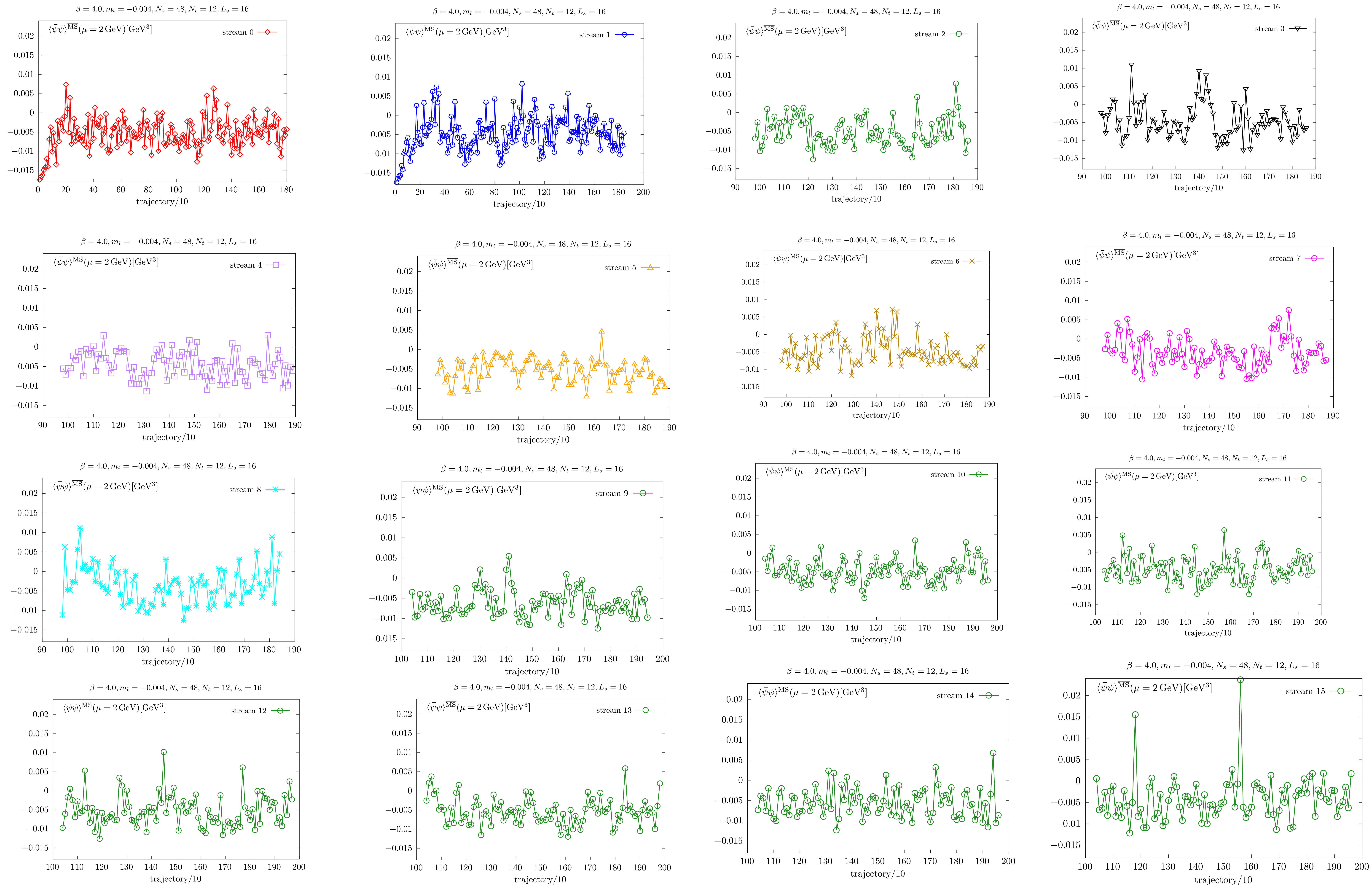

$\beta = 4.0, m_l = -0.004, N_s = 48, N_t = 12, L_s = 16$
$\langle\bar{\psi}\psi\rangle^{\overline{\mathrm{MS}}}(\mu = 2\,\mathrm{GeV})[\mathrm{GeV}^3]$
stream 0
trajectory/10
$\beta = 4.0, m_l = -0.004, N_s = 48, N_t = 12, L_s = 16$
$\langle\bar{\psi}\psi\rangle^{\overline{\mathrm{MS}}}(\mu = 2\,\mathrm{GeV})[\mathrm{GeV}^3]$
stream 1
trajectory/10
$\beta = 4.0, m_l = -0.004, N_s = 48, N_t = 12, L_s = 16$
$\langle\bar{\psi}\psi\rangle^{\overline{\mathrm{MS}}}(\mu = 2\,\mathrm{GeV})[\mathrm{GeV}^3]$
stream 2
trajectory/10
$\beta = 4.0, m_l = -0.004, N_s = 48, N_t = 12, L_s = 16$
$\langle\bar{\psi}\psi\rangle^{\overline{\mathrm{MS}}}(\mu = 2\,\mathrm{GeV})[\mathrm{GeV}^3]$
stream 3
trajectory/10
$\beta = 4.0, m_l = -0.004, N_s = 48, N_t = 12, L_s = 16$
$\langle\bar{\psi}\psi\rangle^{\overline{\mathrm{MS}}}(\mu = 2\,\mathrm{GeV})[\mathrm{GeV}^3]$
stream 4
trajectory/10
$\beta = 4.0, m_l = -0.004, N_s = 48, N_t = 12, L_s = 16$
$\langle\bar{\psi}\psi\rangle^{\overline{\mathrm{MS}}}(\mu = 2\,\mathrm{GeV})[\mathrm{GeV}^3]$
stream 5
trajectory/10
$\beta = 4.0, m_l = -0.004, N_s = 48, N_t = 12, L_s = 16$
$\langle\bar{\psi}\psi\rangle^{\overline{\mathrm{MS}}}(\mu = 2\,\mathrm{GeV})[\mathrm{GeV}^3]$
stream 6
trajectory/10
$\beta = 4.0, m_l = -0.004, N_s = 48, N_t = 12, L_s = 16$
$\langle\bar{\psi}\psi\rangle^{\overline{\mathrm{MS}}}(\mu = 2\,\mathrm{GeV})[\mathrm{GeV}^3]$
stream 7
trajectory/10
$\beta = 4.0, m_l = -0.004, N_s = 48, N_t = 12, L_s = 16$
$\langle\bar{\psi}\psi\rangle^{\overline{\mathrm{MS}}}(\mu = 2\,\mathrm{GeV})[\mathrm{GeV}^3]$
stream 8
trajectory/10
$\beta = 4.0, m_l = -0.004, N_s = 48, N_t = 12, L_s = 16$
$\langle\bar{\psi}\psi\rangle^{\overline{\mathrm{MS}}}(\mu = 2\,\mathrm{GeV})[\mathrm{GeV}^3]$
stream 9
trajectory/10
$\beta = 4.0, m_l = -0.004, N_s = 48, N_t = 12, L_s = 16$
$\langle\bar{\psi}\psi\rangle^{\overline{\mathrm{MS}}}(\mu = 2\,\mathrm{GeV})[\mathrm{GeV}^3]$
stream 10
trajectory/10
$\beta = 4.0, m_l = -0.004, N_s = 48, N_t = 12, L_s = 16$
$\langle\bar{\psi}\psi\rangle^{\overline{\mathrm{MS}}}(\mu = 2\,\mathrm{GeV})[\mathrm{GeV}^3]$
stream 11
trajectory/10
$\beta = 4.0, m_l = -0.004, N_s = 48, N_t = 12, L_s = 16$
$\langle\bar{\psi}\psi\rangle^{\overline{\mathrm{MS}}}(\mu = 2\,\mathrm{GeV})[\mathrm{GeV}^3]$
stream 12
trajectory/10
$\beta = 4.0, m_l = -0.004, N_s = 48, N_t = 12, L_s = 16$
$\langle\bar{\psi}\psi\rangle^{\overline{\mathrm{MS}}}(\mu = 2\,\mathrm{GeV})[\mathrm{GeV}^3]$
stream 13
trajectory/10
$\beta = 4.0, m_l = -0.004, N_s = 48, N_t = 12, L_s = 16$
$\langle\bar{\psi}\psi\rangle^{\overline{\mathrm{MS}}}(\mu = 2\,\mathrm{GeV})[\mathrm{GeV}^3]$
stream 14
trajectory/10
$\beta = 4.0, m_l = -0.004, N_s = 48, N_t = 12, L_s = 16$
$\langle\bar{\psi}\psi\rangle^{\overline{\mathrm{MS}}}(\mu = 2\,\mathrm{GeV})[\mathrm{GeV}^3]$
stream 15
trajectory/10

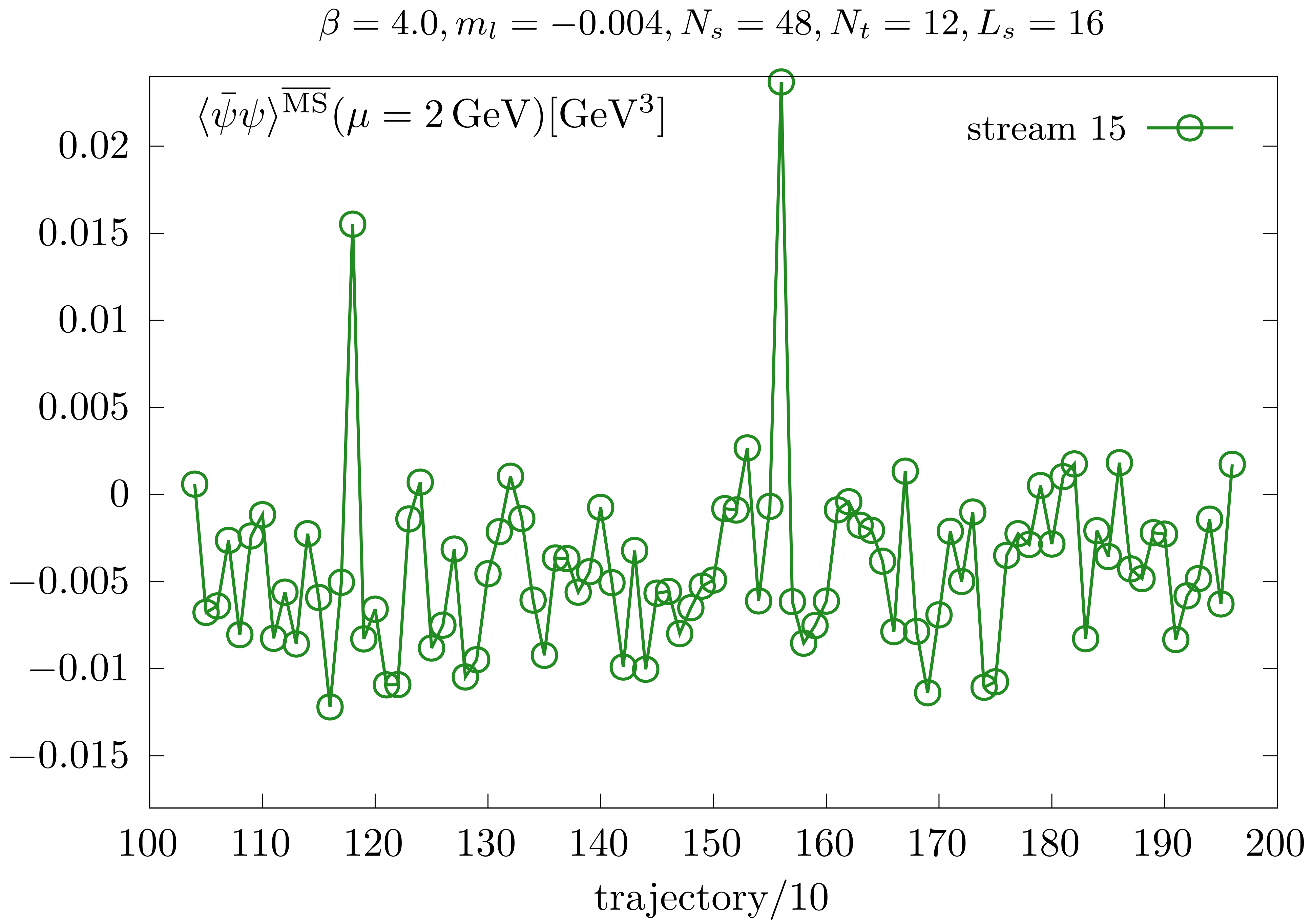
$\beta = 4.0, m_l = -0.004, N_s = 48, N_t = 12, L_s = 16$
$\langle\bar{\psi}\psi\rangle^{\overline{\rm MS}}(\mu = 2\,{\rm GeV})[{\rm GeV}^3]$
stream 15
0.02
0.015
0.01
0.005
0
−0.005
−0.01
−0.015
100 110 120 130 140 150 160 170 180 190 200
trajectory/10

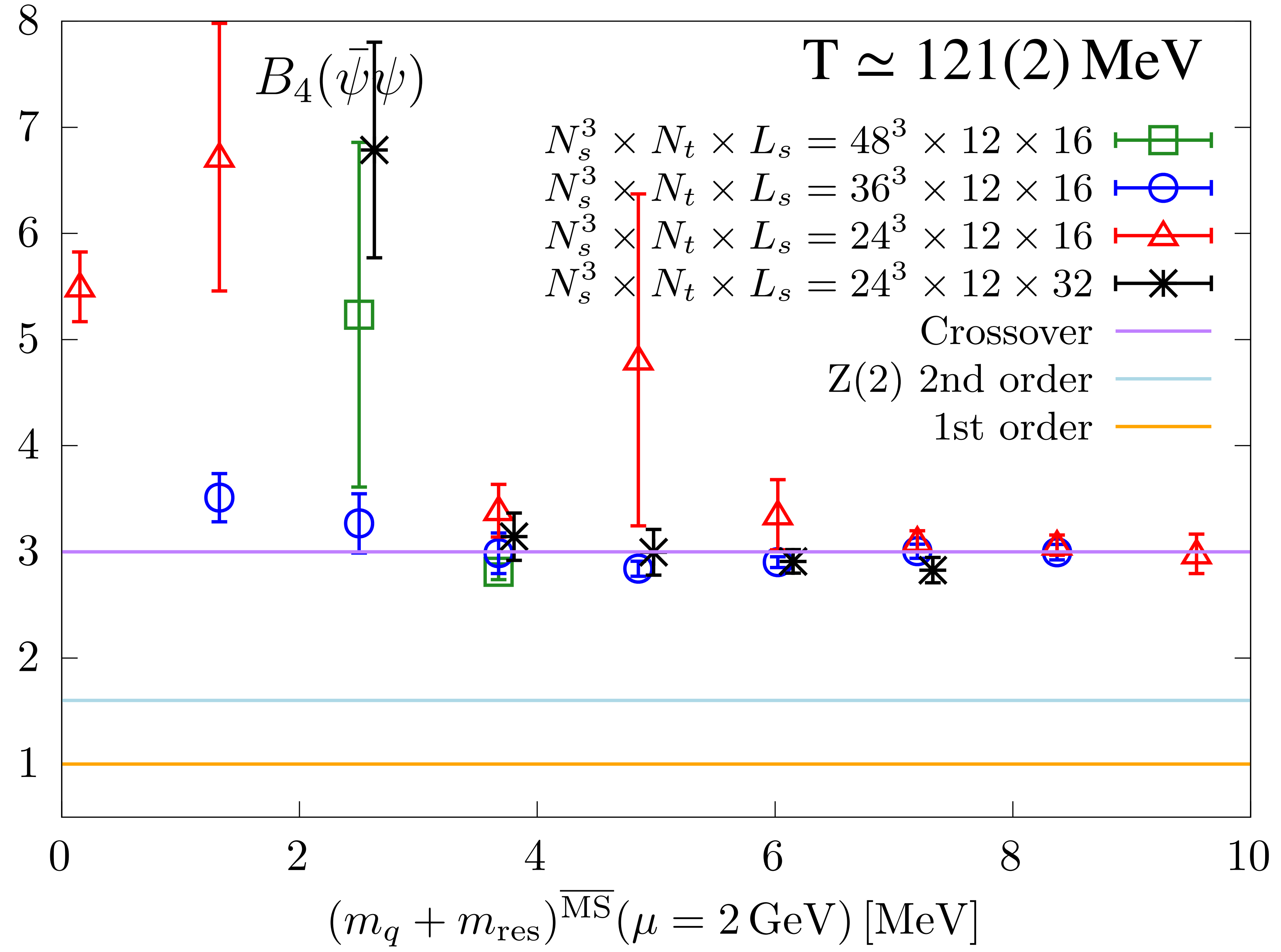
$B_4(\bar{\psi}\psi)$
T ≃ 121(2) MeV
$N_s^3 \times N_t \times L_s = 48^3 \times 12 \times 16$
$N_s^3 \times N_t \times L_s = 36^3 \times 12 \times 16$
$N_s^3 \times N_t \times L_s = 24^3 \times 12 \times 16$
$N_s^3 \times N_t \times L_s = 24^3 \times 12 \times 32$
Crossover
Z(2) 2nd order
1st order
$(m_q + m_{\rm res})^{\overline{\rm MS}}(\mu = 2\,{\rm GeV})$ [MeV]

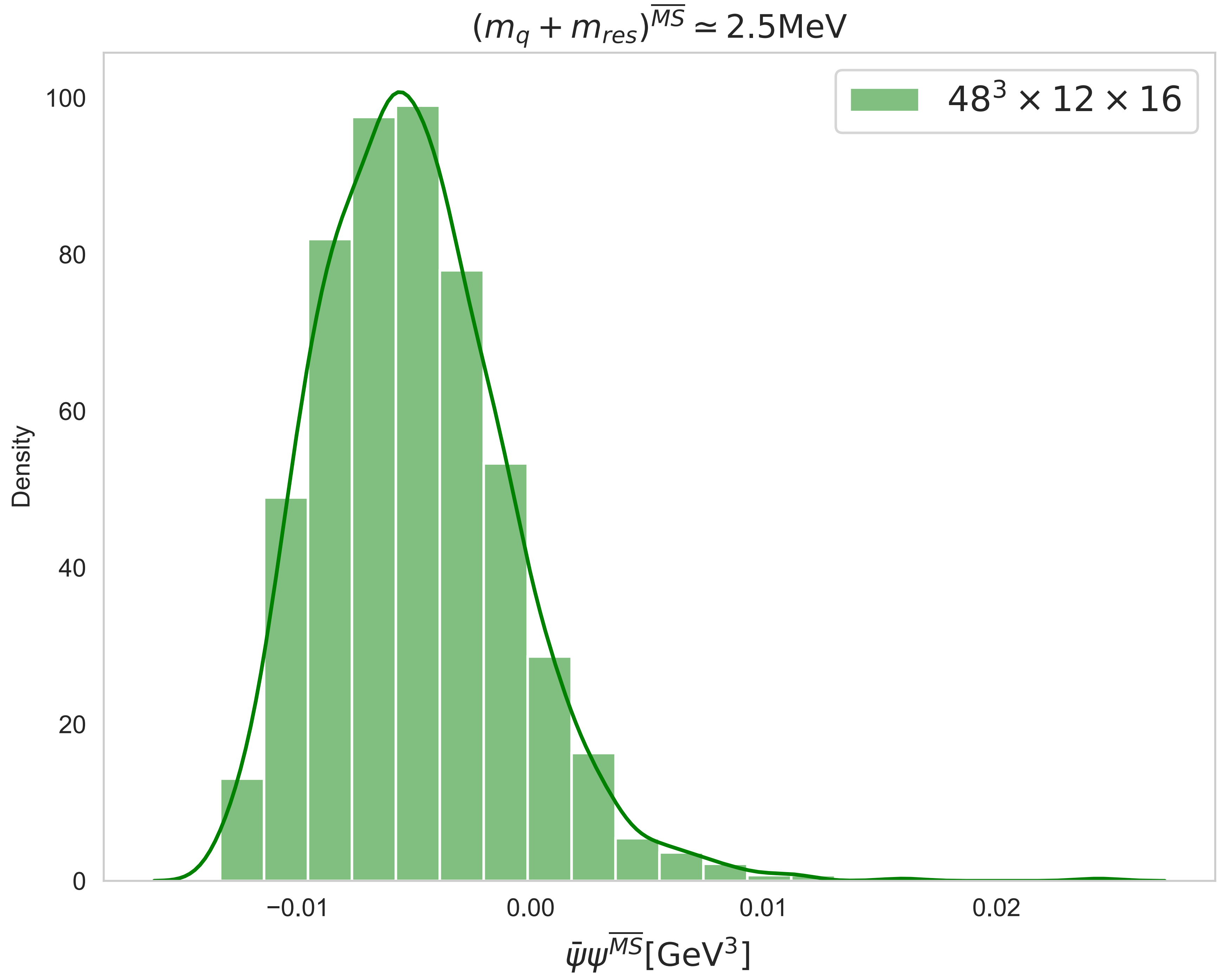
$(m_q + m_{res})^{\overline{MS}} \simeq 2.5$MeV
$48^3 \times 12 \times 16$
Density
0 20 40 60 80 100
−0.01 0.00 0.01 0.02
$\bar{\psi}\psi^{\overline{MS}}[{\rm GeV}^3]$

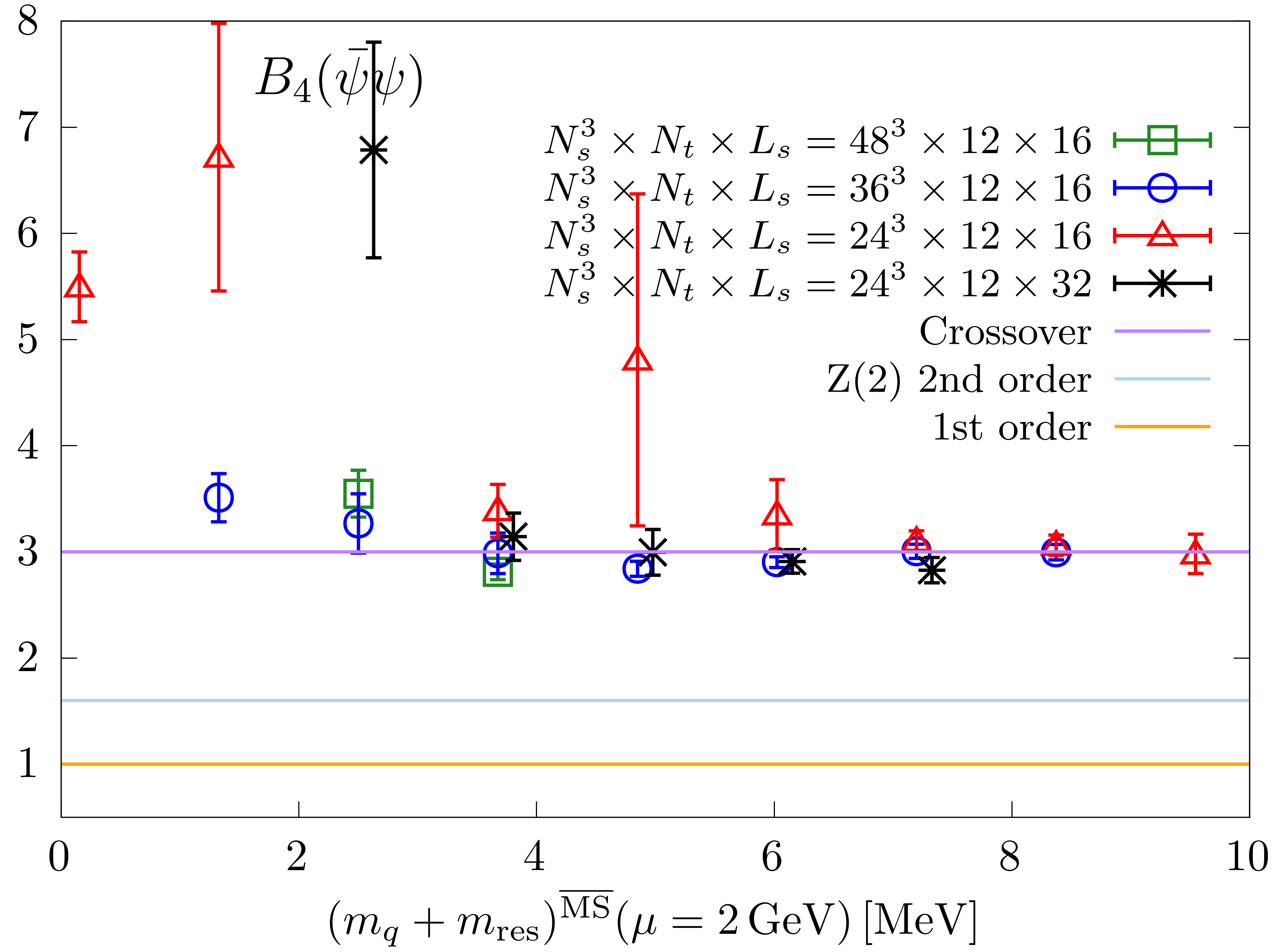
$B_4(\bar{\psi}\psi)$
$N_s^3 \times N_t \times L_s = 48^3 \times 12 \times 16$
$N_s^3 \times N_t \times L_s = 36^3 \times 12 \times 16$
$N_s^3 \times N_t \times L_s = 24^3 \times 12 \times 16$
$N_s^3 \times N_t \times L_s = 24^3 \times 12 \times 32$
Crossover
Z(2) 2nd order
1st order
$(m_q + m_{\rm res})^{\overline{\rm MS}}(\mu = 2\,{\rm GeV})$ [MeV]